



Published in final edited form as:

Neuron. 2009 August 27; 63(4): 466–481. doi:10.1016/j.neuron.2009.08.005.

The cell-intrinsic requirement of Sox6 for cortical interneuron development

Renata Batista-Brito¹, Elsa Rossignol^{1,†}, Jens Hjerling-Leffler^{1,†}, Myrto Denaxa², Michael Wegner³, Véronique Lefebvre⁴, Vassilis Pachnis², and Gord Fishell^{1,§}

¹Neuroscience Program and the Department of Cell Biology, Smilow Research Center, New York University School of Medicine, 522 First Avenue, New York, NY 10016, USA

²Division of Molecular Neurobiology, MRC, National Institute for Medicine Research, Mill Hill, London, UK.

³Institut fuer Biochemie, Universitaet Erlangen-Nuernberg, Fahrstrasse 17, 91054 Erlangen, Germany

⁴Department of Cell Biology and Orthopaedic Research Center, Cleveland Clinic Lerner Research Institute, 9500 Euclid Avenue (NC10), Cleveland, OH 44195, United States

Abstract

We describe the role of Sox6 in cortical interneuron development, from a cellular to a behavioral level. We identify Sox6 as a protein expressed continuously within MGE-derived cortical interneurons from postmitotic progenitor stages into adulthood. Both its expression pattern and null phenotype suggests that *Sox6* gene function is closely linked to that of *Lhx6*. In both *Lhx6* and *Sox6* null animals the expression of PV and SST, as well as the position of both basket and Martinotti neurons are abnormal. We find that Sox6 functions downstream of *Lhx6*. Electrophysiological analysis of *Sox6* mutant cortical interneurons revealed that basket cells, even when mis-positioned, retain characteristic but immature FS physiological features. Our data suggest that Sox6 is not required for the specification of MGE-derived cortical interneurons. It is however, necessary for their normal positioning and maturation. As a consequence, the specific removal of *Sox6* from this population results in a severe epileptic encephalopathy.

Keywords

cortical interneurons; development; genetics; Sox6; Lhx6; Nkx2-1; epilepsy

Introduction

Since the pioneering work of Ramon Y Cajal in the last century, cortical interneuron populations have been recognized to be particularly diverse in terms of their morphology, intrinsic properties and connectivity. This heterogeneity of interneurons subtypes is thought

© 2009 Published by Elsevier Inc.

§Correspondence should be addressed to G.F. (fisheg01@nyumc.org).

[†]These authors contributed equally to this manuscript.

Publisher's Disclaimer: This is a PDF file of an unedited manuscript that has been accepted for publication. As a service to our customers we are providing this early version of the manuscript. The manuscript will undergo copyediting, typesetting, and review of the resulting proof before it is published in its final citable form. Please note that during the production process errors may be discovered which could affect the content, and all legal disclaimers that apply to the journal pertain.

to enable them to contribute differentially to various higher brain functions (Glickfeld et al., 2009; Szabadics et al., 2006; Tamas et al., 2003). During development, cortical interneurons have been implicated in the assembly of cortical networks and the emergent properties of the brain. For instance, one of the earliest coherent forms of brain activity, giant depolarizing potentials is dependent on the activity of GABAergic interneurons (Allene et al., 2008). Efforts to determine the contribution of specific interneuron subtypes to network development have been hampered by the fact that cortical interneuron classification is based on mature properties not yet present during these early events. However, recent findings show that the expression of genetic programs specific for the place and time of origin of the cells correlate with their mature properties (for review see Batista-Brito and Fishell, 2009).

All cortical interneurons, at least in non-primate mammals, are derived from the subpallium of the telencephalon (Corbin et al., 2001; Kriegstein and Noctor, 2004; Marin and Rubenstein, 2001, 2003). In particular, they are believed to arise from two telencephalic transient embryonic structures, the medial and caudal ganglionic eminences (the MGE and CGE, respectively) (Anderson et al., 2001; Nery et al., 2002; Sussel et al., 1999). Fate mapping studies have shown that the cortical interneuron subtypes arising from these two sources are mutually exclusive (Butt et al., 2005; Fogarty et al., 2007; Nery et al., 2002; Xu et al., 2008). While the MGE gives rise to the fast spiking (FS) basket cells and Martinotti interneurons, the CGE is the source of the bipolar and neurogliaform populations (Butt et al., 2005; GF unpublished data). This suggests that distinct genetic programs are initiated within the MGE and CGE interneuron progenitors. Indeed, numerous genes expressed throughout the ventricular and subventricular zones (VZ and SVZ, respectively) appear to contribute to the specification, migration and differentiation of cortical interneuron populations. These include genes with widespread expression throughout the subpallium, such as *Mash1*, the *Dlx* family of genes (*Dlx1,2,5* and *6*) (Anderson et al., 1997a; Anderson et al., 1997b; Cobos et al., 2005; Ghanem et al., 2007; Potter et al., 2009), *Met* (Powell et al., 2001), *Olig2* (Miyoshi et al., 2007b), and *Gsh2* (Corbin et al., 2000; Fogarty et al., 2007; Stenman et al., 2003). As well as, a series of transcription factor-encoding genes with more restricted subpallial regional expression, such as *Nkx2-1* (Butt et al., 2008; Du et al., 2008; Nobrega-Pereira et al., 2008; Sussel et al., 1999; Xu et al., 2008), *Lhx6* (Alifragis et al., 2004; Cobos et al., 2006; Du et al., 2008; Fogarty et al., 2007; Liodis et al., 2007; Zhao et al., 2008), *Lhx7* (Fragkouli et al., 2005; Zhao et al., 2003), *Nkx6.2* (Fogarty et al., 2007; Sousa et al., 2009) and *CoupTFII* (Kanatani et al., 2008; Tripodi et al., 2004). These latter genes are attractive candidates for regulating the specification of particular cortical interneuron subclasses.

In particular, *Nkx2-1* has been shown to repress the program utilized by CGE-derived cortical interneuron populations, while simultaneously promoting the development of MGE-derived cortical interneurons (Butt et al., 2008; Sussel et al., 1999). Recent work suggests that *Lhx6* is an essential downstream effector of *Nkx2-1* activity (Du et al., 2008). In accordance, loss of function analysis of an *Lhx6* null allele indicates that this gene is required for the positioning and maturation of MGE-derived cortical interneuron populations (Liodis et al., 2007; Zhao et al., 2008). However, other effector genes that act downstream of *Nkx2-1* and *Lhx6* have yet to be identified.

In an attempt to better address the molecular mechanisms utilized in the generation of cortical interneuron subclasses, a number of laboratories, including our own, have undertaken genome-wide microarray analyses of the genes expressed within developing cortical interneurons (Batista-Brito et al., 2008; Marsh et al., 2008; Okaty et al., 2009). Through this approach the Sry-related HMG box-containing transcription factor *Sox6* was identified. This gene has been previously implicated as being involved in cell fate commitment in cartilage and oligodendrogenesis, thus suggesting that it might regulate cell fate in interneurons as well. Indeed, a very recently published paper found as we did that *Sox6* is expressed and required

in MGE-derived cortical interneurons, as well as playing an independent role in pallial/subpallial patterning (Azim et al., 2009). In addition, recent work by the same group has identified *Sox5*, a close homolog of *Sox6*, as being required for the specification of deep layer pyramidal neurons in layer V and VI of the cortex (Lai et al., 2008). Here we demonstrate that *Sox6* is present in most if not all MGE-derived neurons in the mature brain and appears to function genetically downstream of *Lhx6*. Moreover we show that *Sox6* is required for the positioning and maturation of FS basket cells and to a lesser extent Martinotti cells. We demonstrate that these cellular abnormalities result in the development of a progressive and severe epileptic encephalopathy.

Results

Migrating cortical interneurons express *Sox6*

We identified *Sox6* in a previous microarray analysis to be expressed in cortical interneurons (Batista-Brito et al., 2008). In order to analyze the expression of *Sox6*, we used the pan-interneuron transgenic line *Dlx5/6^{Cre};RCE^{EGFP/+}*, which allows for the permanent labeling of interneurons with EGFP through Cre-mediated recombination of the RCE reporter. Immunocytochemistry of *Sox6* demonstrated that migrating cortical interneurons express this protein at all of the analyzed time points (E12.5, E13.5: data not shown; E14.5: Figure 1A,a'). Furthermore, *Sox6* is also expressed in other cortical populations, particularly within the ventricular zone (VZ) of the dorsal telencephalon (Figure 1A).

Due to the high degree of similarity between *Sox6* and *Sox5* (Lefebvre et al., 2007; Lai et al., 2008), we tested if *Sox5* was expressed in migrating cortical interneurons (Figure 1B,b'). While *Sox5* is expressed in postmitotic pyramidal cells, it is excluded from cortical interneurons. Indeed, our analysis revealed that *Sox5* and *Sox6* expression is complementary within the neocortex (c.f. Figure 1a' and b').

To determine whether *Sox6* is expressed within a specific subpopulation of cortical interneurons, we used genetic fate-mapping and immunocytochemical co-localization to examine its overlap with *Lhx6*, a marker of MGE-derived cortical interneuronal lineages (Cobos et al., 2006; Du et al., 2008; Fogarty et al., 2007; Liodis et al., 2007), (Figure 1C,D). *Sox6* and *Lhx6* are extensively co-localized within the MGE, with the vast majority of *Lhx6* expressing cells also being *Sox6* positive (Figure 1C: 94±6% based on the colocalization of EGFP and *Sox6* in *Lhx6^{cre} RCE^{EGFP/+}* mice). However, while *Sox6* is highly expressed in post-mitotic migrating interneurons, its level of expression is lower within the MGE (Figure 1d'), in contrast to *Lhx6* whose levels are similar in both proliferative and migrating interneurons (Figure 1d'-d'').

To determine if *Sox6* expressing cells are mitotic, we examined the expression of the proliferation marker Ki-67 (Kill, 1996) (Figure 1E). In the ventral telencephalon only a small percentage of *Sox6* cells were undergoing proliferation within the SVZ (Figure 1e'). In contrast, *Sox6* expressing cells within the cortical VZ uniformly express Ki-67, suggesting that *Sox6* is uniformly expressed in all the progenitors giving rise to pyramidal cell lineages (Figure 1e'').

Sox6 is expressed in mature MGE-derived cortical interneurons

By fate mapping cortical interneurons using the pan-interneuron transgenic labeling strategy *Dlx5/6^{Cre};RCE^{EGFP/+}*, we determined that 62±3% (N=3) of interneurons within the P21 cortex express *Sox6* (Figure 2A). We also detected extensive *Sox6* labeling in hippocampal interneurons (Figure 2B). While the vast majority of *Sox6* cells in the cortex are interneurons, most of the remaining ones express *Olig2* (data not shown).

In the murine somatosensory cortex, parvalbumin (PV), somatostatin (SST) and vasoactive intestinal polypeptide (VIP) are expressed in mutually exclusive populations of cortical interneurons (Kubota et al., 1994; Miyoshi et al., 2007a). By genetic fate mapping it has recently been demonstrated that PV- and SST-expressing interneurons are exclusively derived from the MGE, while VIP cells do not come from that lineage (Fogarty et al., 2007; Xu et al., 2004). By contrast, CR and NPY, label interneuron populations derive from both the MGE and the CGE (Butt et al., 2005; Fogarty et al., 2007; Xu et al., 2004). Hence, we performed co-immunohistochemistry for Sox6 and these interneuron markers (Figure 2C–F, N=3). This analysis revealed that the vast majority of PV- (93±4%) and SST-expressing (94±6%) interneurons are Sox6 positive, while virtually all the VIP interneurons are Sox6 negative (2±1%). Furthermore, we found that 40±4% of NPY, and 19±2% of CR interneurons co-express Sox6. Taken together, these results demonstrate that Sox6 is expressed in most mature MGE-derived interneurons.

Sox6 loss of function

Sox6 null mice are generally born alive, but the majority of them die within an hour of birth from unknown causes (Smits et al., 2001). A very small percentage of *Sox6* null mice live up to P10–11; however, these mice are consistently smaller and weaker than their control littermates. To test the functional role of *Sox6* in cortical interneurons, we began by analyzing the surviving *Sox6* null mice (*Sox6*^{-/-}) at P10–P11. While the total number of cortical interneurons, as assessed by *Gad67* expression was not obviously severely affected (Supplemental Figure 1A,B), the interneuron markers PV and SST appeared to be greatly decreased, while the numbers of NPY expressing cells appeared to be dramatically increased (results not shown). In contrast, VIP-expression was not affected in the *Sox6* mutants. These findings are consistent with a similar analysis examining the role of *Sox6* in these same contexts (Azim et al., 2009).

The most striking of these findings was the loss of PV-expressing cells. However, given the late initiation of expression of this protein (approximately P12 in wildtype cortical basket cells) coupled with the high level of lethality in the mutant, it is difficult to know whether these observations reflect a loss of this population or simply their failure to mature in *Sox6* mutant mice. Hence, we sought to examine the effect of conditional ablation of *Sox6* specifically within the MGE-derived cortical interneuron populations. By using the *Lhx6*^{Cre} driver in combination with a *Sox6*^{F/F} conditionally-null allele we were able to restrict the removal of *Sox6* solely to the MGE-derived population (Fogarty et al., 2007). The intersection of *Lhx6*- and *Sox6*-expression allows for exquisite specificity for testing the function of *Sox6* within cortical interneurons derived from the MGE. By including the *RCE*^{EGFP/+} reporter line in our analysis, we were able to fate map the *Lhx6/Sox6* expressing cells in both controls (*Sox6*^{F/+}; *Lhx6*^{Cre}; *RCE*^{EGFP/+}) and conditional mutants (*Sox6*^{F/F}; *Lhx6*^{Cre}; *RCE*^{EGFP/+}). Moreover, by examining the EGFP-negative cortical interneuron population, we could gauge the non-cell autonomous consequences of loss of *Sox6* on CGE lineages. *Sox6*^{F/F}; *Lhx6*^{Cre}; *RCE*^{EGFP/+} animals generally resembled their non-mutant littermates up to approximately P15. However, they subsequently failed to thrive and developed a severe seizure disorder, ultimately resulting in death between the ages of P17–P19.

Sox6 is necessary for cortical interneuron migration and laminar positioning

Sox6^{F/F}; *Lhx6*^{Cre}; *RCE*^{EGFP/+} mutant cells did not show any obvious defect in tangential migration (c.f Figure 3A–D with Lavdas et al., 1999; Marin and Rubenstein, 2001). Upon reaching the cortex, interneurons shift to a radial mode of migration as they enter the cortical plate (Ang et al., 2003; Polleux et al., 2002). Our data appear to indicate that conditionally null *Sox6* MGE-derived interneurons have a defect in their ability to transition from tangential to radial migration. Consequently they accumulate in the marginal (MZ) and intermediate (IZ)

zone. To provide landmarks for specific cortical laminae, we used the perinatally-expressed transcription factors *Ctip2* (Figure 3 A, B, E,F: which is expressed in layer V and at lower levels in layer IVa; Arlotta et al., 2005; Chen et al., 2008) and *Tbr1* (Figure 3C,D,G,H: which is expressed in layer VIa; Hevner et al., 2001). Postnatally, mutant *Sox6* interneurons (*Sox6^{FF};Lhx6^{Cre};RCE^{EGFP/+}*) accumulate in layers I and VI, apparently at the expense of layers II, III and IV (Figure 3I,J; 4A–D: Layer I: control (0.5±0.3%) vs. mutant (17±6%), Layer II/III: control (20±3%) vs. mutant (15±3%), Layer IV: control (16±3%) vs. mutant (5±3%), Layer V: control (31±4%) vs. mutant (22±5%), and Layer VI: control (28±4%) vs. mutant (36±8%)). This population is normally absent from layer I as shown in control littermates (Figure 3E,G,I; 4). Indeed, normally the only cortical interneurons in this layer are CGE-derived (GF unpublished data) and a small population of NPY interneuron derived from the preoptic area (Gelman et al., 2009). Hence, at P17–P19 although redistributed (Figure 4) the total number of fate-mapped interneurons is only slightly decreased (18%±12% decrease; Figure 3J). The mutant cells do however appear to retain their GABAergic interneuron character, as their expression of *Gad67* persists. However there we did observe a reduction in this population comparable to the observed decrease in fate-mapped neurons (19%±11%, Figure 4G,H).

Sox6 mutant interneurons retain their identity but fail to mature

We next performed double immunostainings for EGFP and multiple molecular markers characteristically expressed by different cortical interneuron subtypes (Fig 4,5, N=5). The most dramatic effects observed in the mutant population were a marked decrease in PV expression (by 94±3%; Figure 4A,B, 5A,G) and a concomitant increase in NPY expression (by 77±6%; Figure 4C–F,I,J, Figure 5C,G). There was also a 30±2% reduction in the SST-expressing fate-mapped population and more specifically a complete loss of the SST/CR double-positive subtype (Figure 5B,D,G). The percentage of fate-mapped interneurons expressing the molecular markers *Kv3.1b* (normally expressed in PV-fast spiking cells at P17) and *Kv3.2* (normally expressed in PV-fast spiking cells and some SST-expressing cells) was also accordingly decreased (Figure 5E,F,G). Furthermore, the levels of these markers in those neurons in which expression persisted were markedly reduced (Figure 5F,G). To ascertain the degree of cell death in conditional *Sox6* mutants compared to control animals we performed caspase 3 cleavage staining at E13.5, P1 and P17. At no age did we observe an obvious difference in apoptosis (results not shown). Consistent with this result, we observed that 93±6% of the weakly PV-expressing cells displaced population in layer I were NPY positive (compared to 4±2% in control animals).

We also examined if there was any change in the number or location of non-MGE-derived interneurons (i.e. *Lhx6*-negative). This was accomplished in both control and conditional *Sox6* mutant animals by determining the number and location of EGFP-negative, VIP-expressing and CR-expressing (SST-negative) interneurons. We observed no overall alteration in these interneuron subtypes in the absence of *Sox6* (Figure 5H).

NPY is upregulated both autonomously and non-autonomously in conditional Sox6 null mutants

We observed that 23±5% of the *Dlx5/6*-expressing population are NPY-positive in control mice. However, when this population is examined in *Sox6* conditional null mice, 72±7% of all interneurons express NPY. In addition, in both control and conditionally null mice, all NPY staining within the cortex is confined to interneurons (i.e EGFP-expressing cell, Figure 4I,J). This observation allowed us to examine NPY expression in both MGE-derived and non-MGE-derived lineages by investigating the expression of NPY in *Sox6^{FF};Lhx6^{Cre};RCE^{EGFP/+}* animals (Figure 4C,D; 5C,G,H). We reasoned that since NPY is confined to the interneuron population, all NPY/EGFP-double positive cells in the cortex of these mice must be MGE-derived, while NPY-positive/EGFP-negative cells are not. NPY expression was strongly

upregulated both autonomously (Fig. 5G, $16\pm 2\%$ in control versus $65\pm 4\%$ in mutants; i.e the percentage of EGFP-expressing cells that are NPY-positive) and non-autonomously (Fig. 5H, $30\pm 3\%$ in control versus $48\pm 5\%$ in mutants; i.e numbers of EGFP-negative/NPY-positive cells per area measured).

Sox6 functions genetically downstream of *Lhx6*

The co-expression of Sox6 and Lhx6 within both the MGE, as well as in the postmitotic cortical interneurons derived from this structure, is near complete. Moreover, *Lhx6* null mice resemble *Sox6* mutants in that MGE-derived cortical interneurons are similarly mis-positioned, die at a comparable age and are deficient in similar cortical interneuron populations (Liodis et al., 2007; Zhao et al., 2008). Taken together this suggests that within MGE-progenitors, there exists a genetic interaction between *Lhx6* and *Sox6*. To test this hypothesis, we analyzed whether the reciprocal loss of *Lhx6* and *Sox6* within MGE-derived lineages affects the other's expression (Figure 6). At E15.5, in contrast to control neurons, MGE-derived *Lhx6* mutant interneurons do not express Sox6, as assessed through Sox6-immunostaining of mice on a *Gad67^{EGFP}* (Tamamaki et al., 2003) background (Figure 6A–B). However, within the cortical VZ the expression of Sox6 was unperturbed (Figure 6b').

To more specifically assess the genetic relationship between these two genes, we examined *Lhx6* heterozygote (*Lhx6^{+/-}*) and homozygote mutant (*Lhx6^{-/-}*) interneurons on a *Nkx2-1^{Cre};R26R^{YFP/+}* background, which allowed us to directly visualize MGE-derived interneuron lineages independent of Lhx6 expression (Figure 6C,D). Using this approach, a similar result was obtained at both P2 (data not shown) and P15 (Figure 6C–E). In *Lhx6* mutant animals, we found that the vast majority of YFP-expressing cortical interneurons lose their expression of Sox6 (an $86\pm 4\%$ decrease in the number of MGE fate-mapped interneurons expressing Sox6 in *Lhx6^{-/-}* compared with *Lhx6^{+/-}* animals). As noted above, in control animals we also observe a population of non-neural cortical cells that co-express Sox6 and Olig2 and the proportion of these double-labeled cells was not affected in *Lhx6* mutants (Figure 6C,D).

In contrast, *Lhx6* expression was not affected in *Sox6* mutants (85 ± 4 in controls and 78 ± 6 in mutant animals, per optical area examined; Figure 6F–N). At E14.5, *Sox6* mutant cortical interneurons (*Dlx5/6^{Cre}* fate-mapped EGFP-expressing cells) express *Lhx6* mRNA (Figure 6F,G) and Lhx6 protein (Figure 6H,I). Furthermore, these cells retain their Lhx6 expression at later ages (Figure 6L–N). Taken together these results indicate that in MGE-derived cortical interneurons although *Lhx6* is required for Sox6 expression, *Sox6* is not necessary for Lhx6 induction or maintenance. This leads us to conclude that *Sox6* functions genetically downstream of *Lhx6*.

Sox5 does not compensate for the loss of Sox6 in cortical interneuron lineages

Given the close homology between *Sox5* and *Sox6*, we were curious to determine whether any functional compensation by Sox5 occurs within cortical interneurons upon loss of *Sox6*. To address this issue specifically within the MGE-derived cortical interneuron populations, we examined whether the expression of Sox5 is cell-autonomously upregulated upon loss of *Sox6*. In these animals, Sox5 maintained a normal pattern of expression, and there was no indication that this protein is upregulated within the MGE-derived cortical interneuron population (Figure 6J–K and data not shown). This is distinct from the findings of a recent paper that shows that *Sox5* is upregulated in the *Sox6* null mouse (Azim et al., 2009). Taken together, these results suggest that at least within *Lhx6* lineages, there is no evidence for compensation by Sox5 in *Sox6* conditional mutants and hence the upregulation of *Sox5* in the absence of normal *Sox6* expression is not obligate.

We were also intrigued to explore the role of *Sox6* within the pallium. To specifically remove *Sox6* from cortical lineages, we bred the *Sox6^{F/F}* conditional allele onto an *Emx1^{Cre}* background (N=3 for control and mutants). We investigated whether the loss of *Sox6* in the pallium had an effect on P21 pyramidal neurons by examining the expression of *SatB2* (Supplemental Figure 2A,B, a marker for callosal projecting pyramidal neurons; Alcamo et al., 2008; Britonova et al., 2008) and *Ctip2* (Supplemental Figure 2C,D, expressed in corticofugal pyramidal neurons; Arlotta et al., 2005; Chen et al., 2008) in these mutants. To determine if the loss of this gene has a non-autonomous effect on cortical interneurons, we also examined these mutants for the expression of PV, SST and NPY at P21 (Supplemental Figure 2E–K). Neither analysis produced evidence that the loss of *Sox6* in the cortical primordium has an effect on cortical development. In addition, we did not observe any overt behavioral phenotype or seizures in these animals (results not shown).

Sox6 mutant FS-basket cells exhibit immature intrinsic properties

The loss of *Sox6* results in the ectopic positioning of *Lhx6*-lineage cells to the periphery of the cortical plate, and to layer I in particular. This provided us with the unique opportunity to record the electrophysiological properties of cells of known subtypes within layers where they do not normally reside. The *Lhx6*-lineage includes all MGE-derived cortical interneurons, and is largely comprised of two main subgroups that express SST and PV, respectively. The latter group contains a rather homogenous population of basket cell interneurons characterized as fast-spiking (FS). Although PV is lost in the majority of *Sox6* mutant interneurons (Figure 4, Figure 5) SST-expression is less affected. We performed whole-cell current clamp recordings of EGFP-labeled cells in layer I of acute brain slices from P14–16 mice, with subsequent post-hoc immunohistochemistry for SST and *Kv3.1b*. All cells (n=4) that proved to be negative for SST possessed a firing pattern that clearly resembled that of wild-type FS-interneurons. *Kv3.1b* expression in these cells while present was strongly reduced compared to controls (Figure 7A,B). The dendritic arbors of these cells were large and highly arborized, and the axons formed the typical “baskets” around the cell somas of neighboring cells (Figure 7C) suggesting that they are relatively mature. In order to assay the maturity and integration of the mutant cells in greater detail, we compared their electrophysiological properties to those of FS cells in layer II/III of control animals (Figure 7D–G and Supplementary Table 1; n=3).

The mutant cells were indistinguishable from the control cells with regards to passive membrane properties, such as resting membrane potential (RMP), input resistance (R_{in}) and membrane constant tau (See Supplementary Table 1). Similarly, the spike and afterhyperpolarization (AHP) kinetics, such as half spike width, AHP time to the lowest point and AHP amplitude were not significantly different. However, the multiple spike dynamics of the mutant cells had a lower max firing rate and a more pronounced intra spike interval (ISI) adaptation (Figure 7E; $p=0.047$ and $p=0.0004$ respectively), and were unable to sustain firing during prolonged (5s) protocols (Figure 7F). Furthermore, mutant cells exhibited a higher firing threshold (Figure 7E $p=0.019$) and more pronounced sag ($7.1\pm 1.5\text{mV}$ vs. $2.9\pm 1.9\text{mV}$; $p=0.020$) during hyperpolarizing steps, collectively suggesting that these cells are retarded in their maturation (Itami et al., 2007; Okaty et al., 2009).

A characteristic of the immature cortex is that the frequency of EPSPs in FS-basket cells increases dramatically during development between P10 and P14 (Okaty et al., 2009). To test whether the ectopically positioned FS interneuron population received normal levels of excitatory input, we held the cells at -72mV for at least 2 minutes and measured the frequency at which they received excitatory input. Perhaps surprisingly, there was no difference between the mutant ectopic cells and the control layer II/III FS-cells (Figure 7G). In conclusion these results suggest that with regards to the mutant cells despite having normal morphology and

receiving appropriate levels of input their electrophysiological properties suggest that maturation of FS cells is impaired in these mutants.

Removal of Sox6 in MGE derived lineages leads to a severe epileptic encephalopathy

Sox6 mutants were undistinguishable from their littermates until approximately 15 days of age, at which point they develop spasticity as evidenced by an abnormal scissoring posture of the limbs when mutants were held by the tail. By P16, they became progressively more withdrawn and developed spontaneous seizures. They died between P17 and P19 of a combination of prolonged seizures and dehydration.

To further assess the seizure phenotype, four mutants (two *Sox6^{F/F}; Dlx5/6^{Cre}* and two *Sox6^{F/F}; Lhx6^{Cre}* were combined as they had indistinguishable phenotypes) and four wild-type controls were monitored daily by video-EEG from P16.

The epileptic phenotype was found to be temporally progressive in all recorded mutants. During early P16, mutants remained able to explore and presented minimal cortical EEG anomalies. They were able to generate background theta rhythms similar to controls, although these were somewhat less well sustained and repeatedly intertwined with slower delta waves (Figure 8A). Already at P16, the interictal trace revealed bilateral synchronous bursts of epileptic activity in the hippocampi characterised by fast polyspikes overlying high amplitude delta waves. This epileptic anomaly was accentuated during slow wave sleep (Figure 8B) and were occasionally accompanied by cortical delta waves or polyspikes, behavioural manifested as slowing or rapid axial myoclonus (Figure 8C). This was followed by the development of generalised seizures (Figure 8D) manifested by an axial myoclonus followed by subtle generalized clonic movements. Epileptic activity during these seizures was most often confined to the cortex, with intermittent recruitment of the hippocampi.

Spectral analysis performed on slow wave sleep epochs at late P16.5 and early P17 illustrated the interictal anomalies described above. Examination of the cortical EEG (M1) revealed increased spectral amplitude in the delta frequency band (228 $\mu\text{V}/\text{Hz}$ in mutants vs 163 $\mu\text{V}/\text{Hz}$ in controls, $n=4$). In addition, epileptic bursts observed in the hippocampi were reflected in spectral analyses as increased spectral amplitude in the delta frequency band (Figure 9B, 292 $\mu\text{V}/\text{Hz}$ in mutants vs 199 $\mu\text{V}/\text{Hz}$ in controls), as well as in the beta (43 $\mu\text{V}/\text{Hz}$ vs 30.8 $\mu\text{V}/\text{Hz}$) and gamma (28 $\mu\text{V}/\text{Hz}$ vs 17 $\mu\text{V}/\text{Hz}$) frequency bands (Figure 9A,C). Notably, the spectral amplitude estimates in CA1 revealed a significant new peak around $25\pm 3\text{Hz}$ in the beta range with a minor peak around $53\pm 3\text{Hz}$ in the gamma range (Figure 9A).

Discussion

In the present study, we describe the role of *Sox6* in cortical interneuron development, and the consequences of its removal, from a cellular to a behavioral level. We identify *Sox6* as a protein expressed continuously within MGE-derived cortical interneurons from postmitotic progenitors into adulthood. Both its expression pattern and null phenotype suggests that *Sox6* gene function is closely related to that of *Lhx6*. The two genes appear to be largely co-expressed in MGE-derived interneuron lineages (Figure 1C,D). Moreover, in both *Lhx6* and *Sox6* null animals the expression of PV basket cells and SST Martinotti neurons is abnormal. Examination of the genetic relationship between these two genes led us to conclude that *Sox6* functions downstream of *Lhx6* (Figure 6). Electrophysiological analysis of *Sox6* mutant cortical interneurons revealed that basket cells, even when mis-positioned, retain characteristic but immature FS physiological features (Figure 8). Taken together, our data suggest that *Sox6* is not required for the specification or maintenance of MGE-derived cortical interneuron subtypes. It is however, necessary for their normal positioning and maturation. As a

consequence, the specific removal of *Sox6* from this population results in severe epileptic encephalopathy.

The autonomous and non-autonomous requirements for *Sox6* in cortical interneuron lineages

In the straight *Sox6* null, we and others (Azim et al., 2009) observed a dramatic loss of PV and SST expression and a concomitant increase in NPY expression. Based on our previous analysis of *Nkx2-1* (Butt et al., 2008), we initially surmised that this result indicated a “class-switching” of PV and SST cells into a NPY subtype. Indeed, this is the conclusion reached by the Macklis group in their recent analysis (Azim et al., 2009). However, our analysis of the NPY-expressing ectopic cells in layer I revealed that they possess low levels of PV- and Kv3.1b-expression and retain FS physiological character, arguing against such a fate-switch. Furthermore, our finding that NPY is also upregulated in cells that have not lost *Sox6*-expression, suggests that the expression of this protein is more related to an ambient increase in cortical activity in these seizure prone animals than as a marker of interneuron subtype. Indeed, it is known that *NPY* mRNA expression is increased in response to neuronal activity (Baraban et al., 1997; Nawa et al., 1995), consistent with the presence of this protein in a variety of cortical interneuron subtypes (Karagiannis et al., 2009). Hence, we hypothesize that the upregulation in NPY-expression that we observe in these mutants may be secondary to the increase in cortical activity that ultimately manifests itself in seizures.

The genetic relationship between *Sox6* and *Lhx6*

Sox6 has been most noted for its requirement for bone and oligodendrocyte development (Smits et al., 2001; Stolt et al., 2006) while *Lhx6* is involved in the formation of limbic circuitry (Choi et al., 2005). Despite these divergent roles, their function appears tightly linked within MGE-derived cortical interneuron lineages. The onset of expression of both these genes appears to be dependent on *Nkx2-1* (Du et al., 2008, data not shown, Figure 1D,d'). Although the expression of SST appears more severely affected in *Lhx6* null mice, the removal of either gene results in a similar loss of markers and mis-positioning of interneurons.

Based on our observations that *Lhx6* expression persists in *Sox6* mutants, while *Sox6* expression is lost in *Lhx6* mutants, it seems likely that *Lhx6* functions genetically upstream of *Sox6*. It is however not known whether *Lhx6* directly binds to the promoter of *Sox6*. Within the embryo as a whole, the colocalization of *Lhx6* and *Sox6* is the exception rather than the rule, as outside the telencephalon *Lhx6* and *Sox6* are found in different tissues. Hence, a direct transcriptional relationship must require ancillary partners for *Lhx6* to initiate *Sox6* expression. Alternatively, *Lhx6* and *Sox6* proteins might physically interact to form a transcription complex that fails to function if either partner is absent. If so, *Lhx6* would be posited to both initiate *Sox6* expression and then subsequently interact functionally with it. Furthermore, given the similarity in their loss of function phenotypes, one might construe that the absence of *Sox6* in *Lhx6* mutants accounts for much of the defects observed. In future experiments it will be interesting to gain a more fine grained understanding of the relative requirement for these two genes in cortical interneuron development.

The physiological and behavioral consequences of *Sox6* removal

The epileptic phenotype observed in conditional removal of *Sox6* resembles other mutants in which MGE-derived interneurons are abnormal, including *Nkx2-1* and *Lhx6* null mice, which also develop spontaneous seizures (Butt et al., 2008). However, the temporal emergence of these anomalies and the relative contribution of the hippocampus and the cortex to seizure development have not been previously evaluated.

These mutants appeared phenotypically normal until P15, revealing that intact MGE-derived interneurons are not initially required for the normal development of animal behavior. However, they subsequently developed a severe seizure disorder. Interestingly, cortical excitatory synaptic inputs normally reach their maximal level at P15 (Okaty et al., 2009). This network activity coincides with developmental changes in PV-expressing FS-interneurons during the third and fourth post-natal week, including the maturation of their intrinsic cell firing properties, the development of perineural nets and an improved reliability of GABA release (Doischer et al., 2008; Okaty et al., 2009). In our analysis, the ectopically located neurons displayed intrinsic physiological characteristics of less mature FS-cells, including an inability to sustain fast firing, greater ISI adaptation and a lack of both perineural nets (data not shown) and PV expression. These two latter properties of FS-cells are crucial in regulating plasticity within the cortex (Pizzorusso et al., 2002; Sugiyama et al., 2008). Specifically, adequate expression of parvalbumin, has been shown to play an important role in pre-synaptic calcium homeostasis, as well as neurotransmitter production and release (Caillard et al., 2000; Rutherford et al., 1997).

At present we cannot definitely say whether the apparent immaturity of the cells is caused by intrinsic genetic changes due to the lack of *Sox6*, or is due to their mis-positioning. The fact that even those cells that are correctly positioned in layer II/III and IV lack PV-expression argues that some of the cellular phenotype is caused by cell-intrinsic loss of *Sox6*. Nevertheless, these findings suggest that correctly located fast-spiking basket cells become crucial to dampen excitation and prevent seizures during the third post-natal week. It is interesting to note that a similar pattern of normal early development followed by abrupt onset of seizures is observed in children with catastrophic childhood epilepsies (Nabbout and Dulac, 2003).

Combined contribution of hippocampus and cortex to the epileptic phenotype

Our analysis reveals that epileptic activity appears in the hippocampus prior to the cortex as early as P16. This is consistent with earlier maturation of hippocampal basket cells (P11) compared to their cortical counterparts (P15–P19) (Nabbout and Dulac, 2003; Okaty et al., 2009). Although minimally symptomatic, this sparse hippocampal epileptic activity may contribute to the induction of persistent epileptic circuits in the hippocampus, as well as possibly in efferent cortical areas (Ben-Ari, 2006). However, it is remarkable that *Sox6* mutants become significantly more symptomatic after independent epileptic activity appears in the cortex, suggesting it may be largely responsible for the severity of the observed epileptic encephalopathy.

The precise contribution of FS basket cells to various cortical oscillations is still being investigated (Bartos et al., 2007; Cardin et al., 2009; Sohal et al., 2009; Wulff et al., 2009). Our analysis reveals that despite gross anomalies in the development of MGE-derived interneuron populations, *Sox6* conditional mutants are able to generate rhythms in all frequency bands. FS basket cells are thought to play an important role in the generation and timing of gamma oscillations (Buhl et al., 2003; Cardin et al., 2009; Hormuzdi et al., 2001; Sohal et al., 2009; Traub et al., 1997; Traub et al., 1996). Nevertheless, gamma oscillations were generated in *SOX6* mutants and particularly increased during epileptic discharges in the hippocampus. Similar rhythms have been reported during seizures in parvalbumin knock-out mice and kainite- induced hippocampal seizures (Medvedev et al., 2000; Schwaller et al., 2004). Moreover, FS basket cells are known to contribute to finer properties of gamma in a task specific manner (Fries et al., 2001; Montgomery et al., 2008; Popa et al., 2009). It will thus be interesting to evaluate how these rhythms are modified in *Sox6* conditional mutants when elicited during more specific tasks in the wake behaving animal.

Experimental Procedures

Animal Handling

All animal handling and maintenance were performed according to the regulations of the Institutional Animal Care and Use Committee of the NYU School of Medicine. The *Dlx5/6^{Cre}* (Stenman et al., 2003), *Lhx6^{Cre}* (Fogarty et al., 2007), *Nkx2.1^{Cre}* (Fogarty et al., 2007), *Sox6^{F/+}* (Dumitriu et al., 2006), *Lhx6^{-/+}* (Liodis et al., 2007), *RCE^{EGFP/+}* (Butt et al., 2008), *Gad67E^{GFP}* (Tamamaki et al., 2003), *Emx1^{Cre}* (Iwasato et al., 2003) and *R26R^{YFP/+}* (Srinivas et al., 2001) transgenic lines were maintained in a mixed background (Swiss Webster and C57/B16), and genotyped as previously described (Butt et al., 2008; Dumitriu et al., 2006; Fogarty et al., 2007; Srinivas et al., 2001; Stenman et al., 2003).

In vivo Sox6 conditional loss of function and fate mapping of cortical interneurons

Male *Sox6^{F/+};Dlx5/6^{Cre}* or *Sox6^{F/+};Lhx6^{Cre}* mice were crossed to *Sox6^{F/F};RCE^{EGFP/EGFP}* females to generate productive *Sox6^{F/+};Dlx5/6^{Cre};RCE^{EGFP/+}* (control); *Sox6^{F/F};Dlx5/6^{Cre};RCE^{EGFP/+}* (mutant); or *Sox6^{F/+};Lhx6^{Cre};RCE^{EGFP/+}* (control); *Sox6^{F/F};Lhx6^{Cre};RCE^{EGFP/+}* (mutant) offspring. Our entire analysis was based on examination of outbred mice. Indeed, preliminary examination of the phenotype resulting from the loss of *Sox6* gene function on mice maintained on a Black 6 inbred background indicated that these animals suffer from a more severe phenotype than we observed in our analysis of outbred mice.

Histology and cell counting

See the supplementary materials for the details of these methods.

Acute *in vitro* cortical slice electrophysiology and morphological reconstruction

Whole cell patch clamp electrophysiological recordings were performed on EGFP-expressing cells in acute brain slices prepared from P14–P16 animals, as previously described (Miyoshi et al., 2007b), with the exception that biocytin, instead of Lucifer yellow, was used in the intracellular solution for filling the cells. For details on these methods and the analysis of intrinsic properties and EPSPs see the supplemental material.

Electroencephalography (EEG) video-monitoring

Animals were recorded daily starting at P16 in 3hours sessions, once or twice daily, and were returned to their home cage between recording sessions. Electroencephalographic signal was acquired at 2000Hz acquisition speed, filtered at HP 0.1 Hz, LP 300Hz, and digitalized using Stellate Harmonie acquisition system with simultaneous video monitoring. Traces were analysed subsequently and spectral analysis was completed using Stellate Harmony EEG software. Spectral analysis was carried using Stellate Harmony Spectrum software. Artefact-free interictal EEG segments during slow wave sleep (defined as prominence of delta waves on cortical EEG recording with absence of movement confirmed by EMG and video) were analysed using Fast-Fourier transformation (FFT 1 second, average of 60 segments) and mean root power (signal amplitude) for each spectral band (as defined in Figure 9A) were compared between mutants and controls. For further details see the supplementary methods.

Supplementary Material

Refer to Web version on PubMed Central for supplementary material.

Acknowledgments

Research in the Fishell laboratory is supported by Grants R01MH068469 and R01NS039007 from the NIMH and the NINDS, respectively, as well as generous support from the Simons Foundation. RB was funded by Fundacao Ciencia e Tecnologia (FCT). ER is funded by the Quebec Health Research Fund (FRSQ). JHL was funded by the Swedish Brain Foundation (Hj rnfonden) postdoctoral grant and is currently an EMBO long-term fellow. We wish to thank Dr. Nicoletta Kessaris for providing the *Lhx6^{Cre}* and *Nkx2-1^{Cre}* Mouse lines; and Frank Costantini for providing the line *R26^{YFP}* line, Takuji Iwasato for his *Emx1^{Cre}* and Yuchio Yanagawa for his generous gift of his *Gad67^{EGFP}* allele. We would like to thank Bernardo Rudy for the generous gift of the antibodies Kv3.1b and Kv3.2. We would also like to thank Lihong Yin for excellent technical help. We thank members of the Fishell laboratory for critically reading this manuscript. We would although like to thank Goichi Miyoshi for generously sharing with us unpublished results.

References

- Alcamo EA, Chirivella L, Dautzenberg M, Dobрева G, Fari nas I, Grosschedl R, McConnell SK. *Satb2* regulates callosal projection neuron identity in the developing cerebral cortex. *Neuron* 2008;57:364–377. [PubMed: 18255030]
- Alifragis P, Liapi A, Parnavelas JG. *Lhx6* regulates the migration of cortical interneurons from the ventral telencephalon but does not specify their GABA phenotype. *Journal of Neuroscience* 2004;24:5643–5648. [PubMed: 15201337]
- Allene C, Cattani A, Ackman JB, Bonifazi P, Aniksztejn L, Ben-Ari Y, Cossart R. Sequential generation of two distinct synapse-driven network patterns in developing neocortex. *Journal of Neuroscience* 2008;28:12851–12863. [PubMed: 19036979]
- Anderson SA, Eisenstat DD, Shi L, Rubenstein JL. Interneuron migration from basal forebrain to neocortex: dependence on *Dlx* genes. [see comment]. *Science* 1997a;278:474–476. [PubMed: 9334308]
- Anderson SA, Marin O, Horn C, Jennings K, Rubenstein JL. Distinct cortical migrations from the medial and lateral ganglionic eminences. *Development* 2001;128:353–363. [PubMed: 11152634]
- Anderson SA, Qiu M, Bulfone A, Eisenstat DD, Meneses J, Pedersen R, Rubenstein JL. Mutations of the homeobox genes *Dlx-1* and *Dlx-2* disrupt the striatal subventricular zone and differentiation of late born striatal neurons. *Neuron* 1997b;19:27–37. [PubMed: 9247261]
- Ang ES Jr, Haydar TF, Gluncic V, Rakic P. Four-dimensional migratory coordinates of GABAergic interneurons in the developing mouse cortex. *Journal of Neuroscience* 2003;23:5805–5815. [PubMed: 12843285]
- Arlotta P, Molyneaux BJ, Chen J, Inoue J, Kominami R, Macklis JD. Neuronal subtype-specific genes that control corticospinal motor neuron development in vivo. *Neuron* 2005;45:207–221. [PubMed: 15664173]
- Azim E, Jabaudon D, Fame RM, Macklis JD. *SOX6* controls dorsal progenitor identity and interneuron diversity during neocortical development. *Nat Neurosci* 2009 Aug 5;2009[Epub ahead of print]
- Baraban SC, Hoppeler G, Erickson JC, Schwartzkroin PA, Palmiter RD. Knock-out mice reveal a critical antiepileptic role for neuropeptide Y. *Journal of Neuroscience* 1997;17:8927–8936. [PubMed: 9364040]
- Bartos M, Vida I, Jonas P. Synaptic mechanisms of synchronized gamma oscillations in inhibitory interneuron networks. *Nature Reviews Neuroscience* 2007;8:45–56.
- Batista-Brito R, Machold R, Klein C, Fishell G. Gene expression in cortical interneuron precursors is prescient of their mature function. *Cerebral Cortex* 2008;18:2306–2317. [PubMed: 18250082]
- Ben-Ari Y. Basic developmental rules and their implications for epilepsy in the immature brain. *Epileptic Disorders* 2006;8:91–102. [PubMed: 16793570]
- Britanova O, de Juan Romero C, Cheung A, Kwan KY, Schwark M, Gyorgy A, Vogel T, Akopov S, Mitkovski M, Agoston D, Sestan N, Moln r Z, Tarabykin V. *Satb2* is a postmitotic determinant for upper-layer neuron specification in the neocortex. *Neuron* 2008;57:378–392. [PubMed: 18255031]
- Buhl DL, Harris KD, Hormuzdi SG, Monyer H, Buzsaki G. Selective impairment of hippocampal gamma oscillations in connexin-36 knock-out mouse in vivo. *Journal of Neuroscience* 2003;23:1013–1018. [PubMed: 12574431]

- Butt SJ, Fuccillo M, Nery S, Noctor S, Kriegstein A, Corbin JG, Fishell G. The temporal and spatial origins of cortical interneurons predict their physiological subtype.[see comment]. *Neuron* 2005;48:591–604. [PubMed: 16301176]
- Butt SJ, Sousa VH, Fuccillo MV, Hjerling-Leffler J, Miyoshi G, Kimura S, Fishell G. The requirement of *Nkx2-1* in the temporal specification of cortical interneuron subtypes.[see comment]. *Neuron* 2008;59:722–732. [PubMed: 18786356]
- Caillard O, Moreno H, Schwaller B, Llano I, Celio MR, Marty A. Role of the calcium-binding protein parvalbumin in short-term synaptic plasticity. *Proc Natl Acad Sci U S A* 2000;97:13372–13377. [PubMed: 11069288]
- Cardin JA, Carlen M, Meletis K, Knoblich U, Zhang F, Deisseroth K, Tsai LH, Moore CI. Driving fast-spiking cells induces gamma rhythm and controls sensory responses. *Nature* 2009;459:663–667. [PubMed: 19396156]
- Chen B, Wang SS, Hattox AM, Rayburn H, Nelson SB, McConnell SK. The *Fezf2-Ctip2* genetic pathway regulates the fate choice of subcortical projection neurons in the developing cerebral cortex. *Proc Natl Acad Sci U S A* 2008;105:11382–11387. [PubMed: 18678899]
- Choi GB, Dong HW, Murphy AJ, Valenzuela DM, Yancopoulos GD, Swanson LW, Anderson DJ. *Lhx6* delineates a pathway mediating innate reproductive behaviors from the amygdala to the hypothalamus.[see comment]. *Neuron* 2005;46:647–660. [PubMed: 15944132]
- Cobos I, Calcagnotto ME, Vilaythong AJ, Thwin MT, Noebels JL, Baraban SC, Rubenstein JL. Mice lacking *Dlx1* show subtype-specific loss of interneurons, reduced inhibition and epilepsy.[see comment]. *Nature Neuroscience* 2005;8:1059–1068.
- Cobos I, Long JE, Thwin MT, Rubenstein JL. Cellular patterns of transcription factor expression in developing cortical interneurons. *Cerebral Cortex* 2006;16:i82–i88. [PubMed: 16766712]
- Corbin JG, Gaiano N, Machold RP, Langston A, Fishell G. The *Gsh2* homeodomain gene controls multiple aspects of telencephalic development. *Development* 2000;127:5007–5020. [PubMed: 11060228]
- Corbin JG, Nery S, Fishell G. Telencephalic cells take a tangent: non-radial migration in the mammalian forebrain. *Nature Neuroscience* 2001;4:1177–1182.
- Doischer D, Hosp JA, Yanagawa Y, Obata K, Jonas P, Vida I, Bartos M. Postnatal differentiation of basket cells from slow to fast signaling devices. *Journal of Neuroscience* 2008;28:12956–12968. [PubMed: 19036989]
- Du T, Xu Q, Ocbina PJ, Anderson SA. *NKX2-1* specifies cortical interneuron fate by activating *Lhx6*. *Development* 2008;135:1559–1567. [PubMed: 18339674]
- Dumitriu B, Dy P, Smits P, Lefebvre V. Generation of mice harboring a *Sox6* conditional null allele. *Genesis: the Journal of Genetics & Development* 2006;44:219–224.
- Fogarty M, Grist M, Gelman D, Marin O, Pachnis V, Kessaris N. Spatial genetic patterning of the embryonic neuroepithelium generates GABAergic interneuron diversity in the adult cortex. *Journal of Neuroscience* 2007;27:10935–10946. [PubMed: 17928435]
- Fragkouli A, Hearn C, Errington M, Cooke S, Grigoriou M, Bliss T, Stylianopoulou F, Pachnis V. Loss of forebrain cholinergic neurons and impairment in spatial learning and memory in *LHX7*-deficient mice. *European Journal of Neuroscience* 2005;21:2923–2938. [PubMed: 15978004]
- Fries P, Reynolds JH, Rorie AE, Desimone R. Modulation of oscillatory neuronal synchronization by selective visual attention. *Science* 2001;291:1560–1563. [PubMed: 11222864]
- Gelman DM, Martini FJ, Nóbrega-Pereira S, Pierani A, Kessaris N, Marín O. The embryonic preoptic area is a novel source of cortical GABAergic interneurons. *Journal of Neuroscience* 2009;29:9380–9389. [PubMed: 19625528]
- Ghanem N, Yu M, Long J, Hatch G, Rubenstein JL, Ekker M. Distinct cis-regulatory elements from the *Dlx1/Dlx2* locus mark different progenitor cell populations in the ganglionic eminences and different subtypes of adult cortical interneurons. *Journal of Neuroscience* 2007;27:5012–5022. [PubMed: 17494687]
- Glickfeld LL, Roberts JD, Somogyi P, Scanziani M. Interneurons hyperpolarize pyramidal cells along their entire somatodendritic axis. *Nature Neuroscience* 2009;12:21–23.
- Hanashima C, Li SC, Shen L, Lai E, Fishell G. *Foxg1* suppresses early cortical cell fate.[see comment]. *Science* 2004;303:56–59. [PubMed: 14704420]

- Hevner RF, Shi YL, Justice N, Hsueh Y, Sheng M, Smiga S, Bulfone A, Goffinet AM, Campagnoni AT, Rubenstein JL. Tbr1 regulates differentiation of the preplate and layer 6. *Neuron* 2:353–366.
- Hormuzdi SG, Pais I, LeBeau FE, Towers SK, Rozov A, Buhl EH, Whittington MA, Monyer H. Impaired electrical signaling disrupts gamma frequency oscillations in connexin 36-deficient mice. [see comment]. *Neuron* 2001;31:487–495. [PubMed: 11516404]
- Itami C, Kimura F, Nakamura S. Brain-derived neurotrophic factor regulates the maturation of layer 4 fast-spiking cells after the second postnatal week in the developing barrel cortex. *Journal of Neuroscience* 2007;27:2241–2252. [PubMed: 17329421]
- Iwasato T, Nomura R, Ando R, Ikeda T, Tanaka M, Itoharu S. Dorsal telencephalon-specific expression of Cre recombinase in PAC transgenic mice. *Genesis* 2004;38:130–138. [PubMed: 15048810]
- Kanatani S, Yozu M, Tabata H, Nakajima K. COUP-TFII is preferentially expressed in the caudal ganglionic eminence and is involved in the caudal migratory stream. *Journal of Neuroscience* 2008;28:13582–13591. [PubMed: 19074032]
- Karagiannis A, Gallopin T, David C, Battaglia D, Geoffroy H, Rossier J, Hillman EM, Staiger JF, Cauli B. Classification of NPY-expressing neocortical interneurons. *Journal of Neuroscience* 2009;29:3642–3659. [PubMed: 19295167]
- Kawaguchi Y. Physiological subgroups of nonpyramidal cells with specific morphological characteristics in layer II/III of rat frontal cortex. *J Neurosci* 1995;15:2638–2655. [PubMed: 7722619]
- Kill IR. Localisation of the Ki-67 antigen within the nucleolus. Evidence for a fibrillar-deficient region of the dense fibrillar component. *Journal of Cell Science* 1996;109:1253–1263. [PubMed: 8799815]
- Kriegstein AR, Noctor SC. Patterns of neuronal migration in the embryonic cortex. *Trends in Neurosciences* 2004;27:392–399. [PubMed: 15219738]
- Kubota Y, Hattori R, Yui Y. Three distinct subpopulations of GABAergic neurons in rat frontal agranular cortex. *Brain Res* 1994;649:159–173. [PubMed: 7525007]
- Lai T, Jabaudon D, Molyneaux BJ, Azim E, Arlotta P, Menezes JR, Macklis JD. SOX5 controls the sequential generation of distinct corticofugal neuron subtypes. *Neuron* 2008;57:232–247. [PubMed: 18215621]
- Lavdas AA, Grigoriou M, Pachnis V, Parnavelas JG. The medial ganglionic eminence gives rise to a population of early neurons in the developing cerebral cortex. *Journal of Neuroscience* 1999;19:7881–7888. [PubMed: 10479690]
- Lefebvre V, Dumitriu B, Penzo-Mendez A, Han Y, Pallavi B. Control of cell fate and differentiation by Sry-related high-mobility-group box (Sox) transcription factors. *International Journal of Biochemistry & Cell Biology* 2007;39:2195–2214. [PubMed: 17625949]
- Liodis P, Denaxaq M, Grigoriou M, Akufu-Addo C, Yanagawa Y, Pachnis V. Lhx6 activity is required for the normal migration and specification of cortical interneuron subtypes. *Journal of Neuroscience* 2007;27:3078–3089. [PubMed: 17376969]
- Marin O, Rubenstein JL. A long, remarkable journey: tangential migration in the telencephalon. *Nature Reviews Neuroscience* 2001;2:780–790.
- Marin O, Rubenstein JL. Cell migration in the forebrain. *Annual Review of Neuroscience* 2003;26:441–483.
- Marsh ED, Minarcik J, Campbell K, Brooks-Kayal AR, Golden JA. FACS-array gene expression analysis during early development of mouse telencephalic interneurons. *Developmental Neurobiology* 2008;68:434–445. [PubMed: 18172891]
- Medvedev A, Mackenzie L, Hiscock JJ, Willoughby JO. Kainic acid induces distinct types of epileptiform discharge with differential involvement of hippocampus and neocortex. *Brain Research Bulletin* 2000;52:89–98. [PubMed: 10808078]
- Miyoshi G, Butt SJ, Takebayashi H, Fishell G. Physiologically distinct temporal cohorts of cortical interneurons arise from telencephalic Olig2-expressing precursors. *J Neurosci* 2007a;27:7786–7798. [PubMed: 17634372]
- Miyoshi G, Butt SJ, Takebayashi H, Fishell G. Physiologically distinct temporal cohorts of cortical interneurons arise from telencephalic Olig2-expressing precursors. *Journal of Neuroscience* 2007b;27:7786–7798. [PubMed: 17634372]

- Montgomery SM, Sirota A, Buzsaki G. Theta and gamma coordination of hippocampal networks during waking and rapid eye movement sleep. *Journal of Neuroscience* 2008;28:6731–6741. [PubMed: 18579747]
- Nabbout R, Dulac O. Epileptic encephalopathies: a brief overview. *Journal of Clinical Neurophysiology* 2003;20:393–397. [PubMed: 14734929]
- Nawa H, Carnahan J, Gall C. BDNF protein measured by a novel enzyme immunoassay in normal brain and after seizure: partial disagreement with mRNA levels. *Eur J Neurosci* 1995;7:1527–1535. [PubMed: 7551179]
- Nery S, Fishell G, Corbin JG. The caudal ganglionic eminence is a source of distinct cortical and subcortical cell populations. *Nature Neuroscience* 2002;5:1279–1287.
- Nobrega-Pereira S, Kessaris N, Du T, Kimura S, Anderson SA, Marin O. Postmitotic Nkx2-1 controls the migration of telencephalic interneurons by direct repression of guidance receptors.[see comment]. *Neuron* 2008;59:733–745. [PubMed: 18786357]
- Okaty BW, Miller MN, Sugino K, Hempel CM, Nelson SB. Transcriptional and electrophysiological maturation of neocortical fast-spiking GABAergic interneurons. *Journal of Neuroscience* 2009;29:7040–7052. [PubMed: 19474331]
- Pizzorusso T, Medini P, Berardi N, Chierzi S, Fawcett JW, Maffei L. Reactivation of ocular dominance plasticity in the adult visual cortex. *Science* 2002;298:1248–1251. [PubMed: 12424383]
- Polleux F, Whitford KL, Dijkhuizen PA, Vitalis T, Ghosh A. Control of cortical interneuron migration by neurotrophins and PI3-kinase signaling. *Development* 2002;129:3147–3160. [PubMed: 12070090]
- Popa D, Popescu AT, Pare D. Contrasting activity profile of two distributed cortical networks as a function of attentional demands. *Journal of Neuroscience* 2009;29:1191–1201. [PubMed: 19176827]
- Potter GB, Petryniak MA, Shevchenko E, McKinsey GL, Ekker M, Rubenstein JL. Generation of Cre-transgenic mice using Dlx1/Dlx2 enhancers and their characterization in GABAergic interneurons. *Molecular & Cellular Neurosciences* 2009;40:167–186. [PubMed: 19026749]
- Powell EM, Mars WM, Levitt P. Hepatocyte growth factor/scatter factor is a motogen for interneurons migrating from the ventral to dorsal telencephalon. *Neuron* 2001;30:79–89. [PubMed: 11343646]
- Rutherford LC, DeWan A, Lauer HM, Turrigiano GG. Brain-derived neurotrophic factor mediates the activity-dependent regulation of inhibition in neocortical cultures. *Journal of Neuroscience* 1997;17:4527–4535. [PubMed: 9169513]
- Schwaller B, Tetko IV, Tandon P, Silveira DC, Vreugdenhil M, Henzi T, Potier MC, Celio MR, Villa AE. Parvalbumin deficiency affects network properties resulting in increased susceptibility to epileptic seizures. *Molecular & Cellular Neurosciences* 2004;25:650–663. [PubMed: 15080894]
- Smits P, Li P, Mandel J, Zhang Z, Deng JM, Behringer RR, de Crombrughe B, Lefebvre V. The transcription factors L-Sox5 and Sox6 are essential for cartilage formation. *Developmental Cell* 2001;1:277–290. [PubMed: 11702786]
- Sohal VS, Zhang F, Yizhar O, Deisseroth K. Parvalbumin neurons and gamma rhythms enhance cortical circuit performance. *Nature* 2009;459:698–702. [PubMed: 19396159]
- Sousa VH, Miyoshi G, Hjerling-Leffler J, Karayannis T, Fishell G. Characterization of Nkx6-2-derived neocortical interneuron lineages. *Cereb Cortex* 2009;19:i1–i10. [PubMed: 19363146]
- Srinivas S, Watanabe T, Lin CS, William CM, Tanabe Y, Jessell TM, Costantini F. Cre reporter strains produced by targeted insertion of EYFP and ECFP into the ROSA26 locus. *BMC Developmental Biology* 2001;1:4. [PubMed: 11299042]
- Stenman J, Toresson H, Campbell K. Identification of two distinct progenitor populations in the lateral ganglionic eminence: implications for striatal and olfactory bulb neurogenesis. *Journal of Neuroscience* 2003;23:167–174. [PubMed: 12514213]
- Stolt CC, Schlierf A, Lommes P, Hillgartner S, Werner T, Kosian T, Sock E, Kessaris N, Richardson WD, Lefebvre V, Wegner M. SoxD proteins influence multiple stages of oligodendrocyte development and modulate SoxE protein function. *Developmental Cell* 2006;11:697–709. [PubMed: 17084361]
- Sugiyama S, Di Nardo AA, Aizawa S, Matsuo I, Volovitch M, Prochiantz A, Hensch TK. Experience-dependent transfer of Otx2 homeoprotein into the visual cortex activates postnatal plasticity. *Cell* 2008;134:508–520. [PubMed: 18692473]

- Sussel L, Marin O, Kimura S, Rubenstein JL. Loss of Nkx2-1 homeobox gene function results in a ventral to dorsal molecular respecification within the basal telencephalon: evidence for a transformation of the pallidum into the striatum. *Development* 1999;126:3359–3370. [PubMed: 10393115]
- Szabadics J, Varga C, Molnar G, Olah S, Barzo P, Tamas G. Excitatory effect of GABAergic axo-axonic cells in cortical microcircuits. *Science* 2006;311:233–235. [PubMed: 16410524]
- Tamamaki N, Yanagawa Y, Tomioka R, Miyazaki J, Obata K, Kaneko T. Green fluorescent protein expression and colocalization with calretinin, parvalbumin, and somatostatin in the GAD67-GFP knock-in mouse. *J Comp Neurol* 2003;467:60–79.
- Tamas G, Lorincz A, Simon A, Szabadics J. Identified sources and targets of slow inhibition in the neocortex. *Science* 2003;299:1902–1905. [PubMed: 12649485]
- Traub RD, Jefferys JG, Whittington MA. Simulation of gamma rhythms in networks of interneurons and pyramidal cells. *J Comput Neurosci* 1997;4:141–150. [PubMed: 9154520]
- Traub RD, Whittington MA, Stanford IM, Jefferys JG. A mechanism for generation of long-range synchronous fast oscillations in the cortex. *Nature* 1996;383:621–624. [PubMed: 8857537]
- Tripodi M, Filosa A, Armentano M, Studer M. The COUP-TF nuclear receptors regulate cell migration in the mammalian basal forebrain. *Development* 2004;131:6119–6129. [PubMed: 15548577]
- Weiser M, Bueno E, Sekirnjak C, Martone ME, Baker H, Hillman D, Chen S, Thornhill W, Ellisman M, Rudy B. The potassium channel subunit KV3.1b is localized to somatic and axonal membranes of specific populations of CNS neurons. *Journal of Neuroscience* 1995;15:4298–4314. [PubMed: 7790912]
- Wulff P, Ponomarenko AA, Bartos M, Korotkova TM, Fuchs EC, Bahner F, Both M, Tort AB, Kopell NJ, Wisden W, Monyer H. Hippocampal theta rhythm and its coupling with gamma oscillations require fast inhibition onto parvalbumin-positive interneurons. *Proceedings of the National Academy of Sciences of the United States of America* 2009;106:3561–3566. [PubMed: 19204281]
- Xu Q, Cobos I, De La Cruz E, Rubenstein JL, Anderson SA. Origins of cortical interneuron subtypes. *Journal of Neuroscience* 2004;24:2612–2622. [PubMed: 15028753]
- Xu Q, Tam M, Anderson SA. Fate mapping Nkx2-1-lineage cells in the mouse telencephalon. *Journal of Comparative Neurology* 2008;506:16–29. [PubMed: 17990269]
- Zhao Y, Flandin P, Long JE, Cuesta MD, Westphal H, Rubenstein JL. Distinct molecular pathways for development of telencephalic interneuron subtypes revealed through analysis of Lhx6 mutants. *Journal of Comparative Neurology* 2008;510:79–99. [PubMed: 18613121]
- Zhao Y, Marin O, Hermes E, Powell A, Flames N, Palkovits M, Rubenstein JL, Westphal H. The LIM-homeobox gene Lhx8 is required for the development of many cholinergic neurons in the mouse forebrain. *Proceedings of the National Academy of Sciences of the United States of America* 2003;100:9005–9010. [PubMed: 12855770]

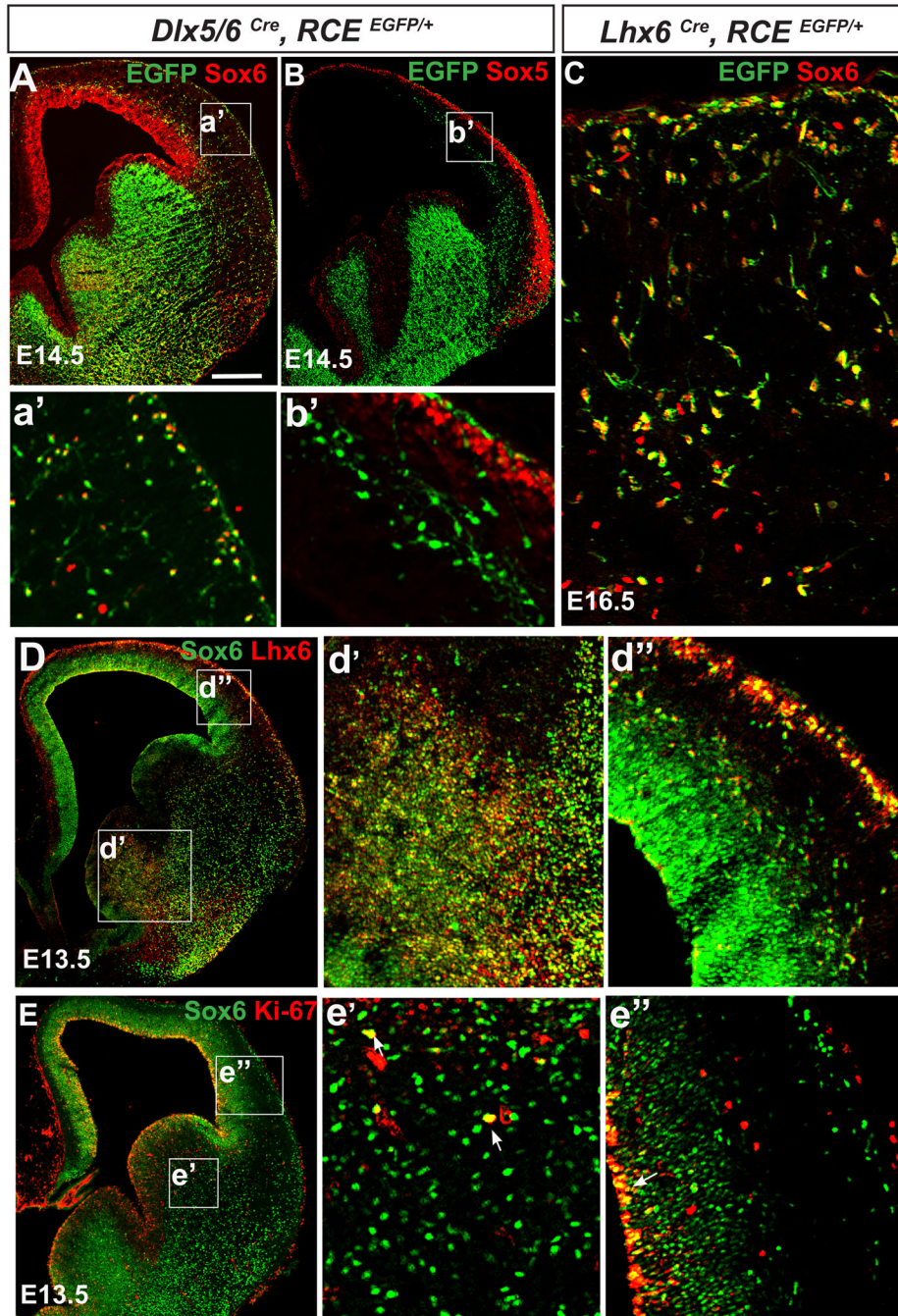


Figure 1. Sox6 is primarily expressed in postmitotic Lhx6-expressing cortical interneurons
 (A) To assess if migrating cortical interneurons express Sox6, coronal telencephalic sections from *Dlx5/6^{Cre};RCE^{EGFP/+}* mice were analyzed at E14.5. (A) Sox6 (red), EGFP (green) double labeled cells were observed in the mantle of the ventral telencephalon. Many of the interneurons in the cortex with morphologies suggesting active migration express Sox6, however some Sox6 expressing cells do not express EGFP (for details see a'). The dorsal ventricular zone also expresses Sox6. (B) In contrast, 'migrating' cortical interneurons do not express Sox5. (C) To assess if Sox6 (red) is expressed within the MGE derived lineage, we fate mapped MGE interneurons using the *Lhx6^{Cre};RCE^{EGFP/+}* (green) line. Virtually all *Lhx6* lineage cortical interneurons express Sox6 (94±6%). (D) The extent of colocalization of Sox6 (green) and Lhx6

(red) was also analyzed by antibody staining at E13.5. Consistent with our genetic fate-mapping of this population, most (if not all) *Lhx6* cells are also *Sox6*-positive, however the relative levels of expression of these two proteins varies. *Sox6*, while expressed at low levels in the MGE (d'), becomes highly expressed in migrating interneurons within the mantle and the cortex (d''). (E) To test if *Sox6* cells are actively proliferating, we examined whether there exists coexpression of *Sox6* (green) and the proliferation marker *Ki-67* (red). Within the ventral telencephalon, while a few cells were double-positive (arrowheads in e'), indicating proliferation, most of the *Sox6* cells did not express *Ki-67*. In the cortex (e'), *Sox6* colocalizes with *Ki-67* exclusively in the ventricular zone (arrow in e''). a'-e'' corresponds to the area outlined by the white squares in A-E respectively. N=3 for each experiment condition. Scale bar in (A) corresponds to 400µm in A-B, 40µm in C, 500µm in D-E.

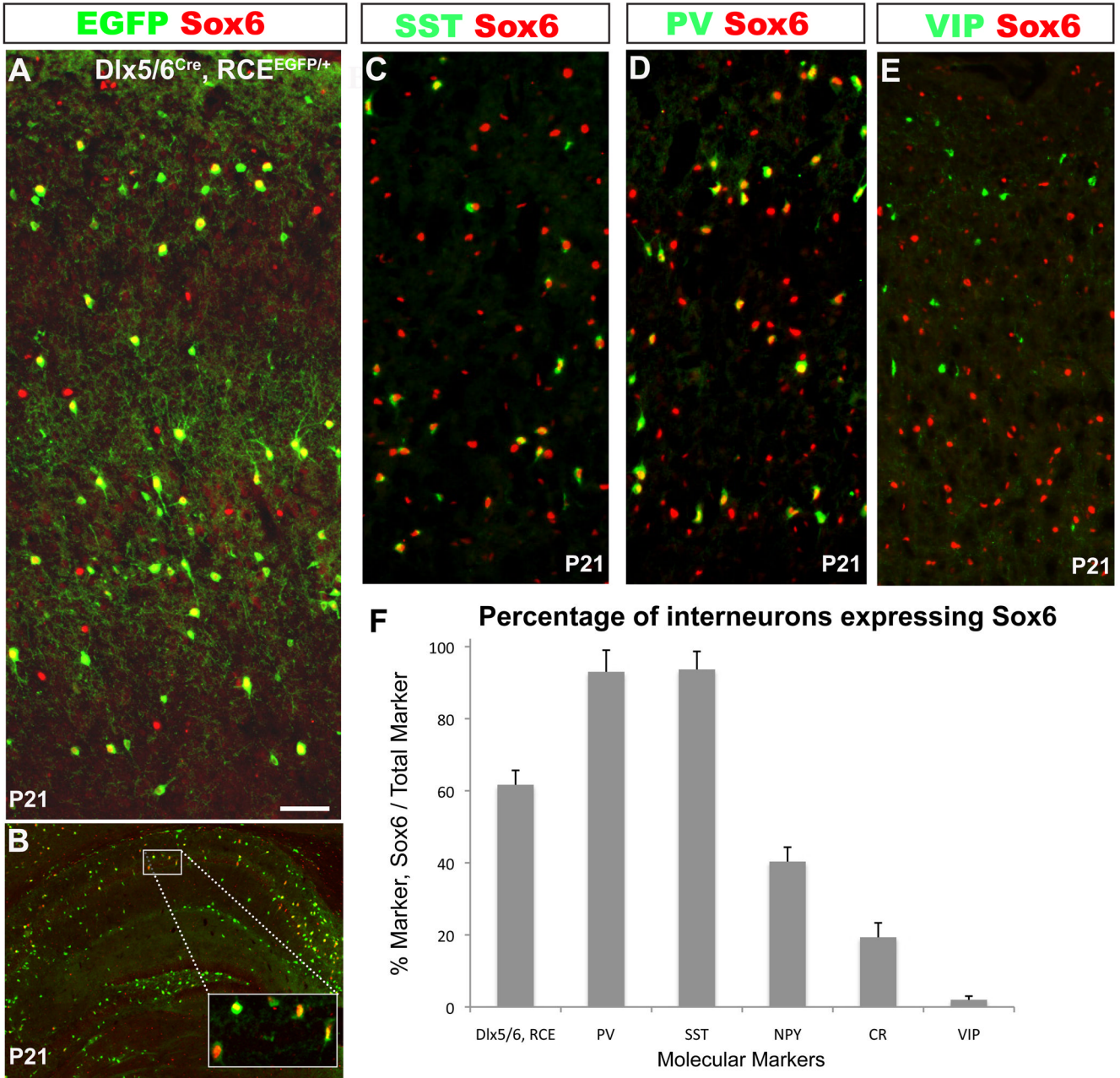


Figure 2. Sox 6 is expressed in mature MGE-derived cortical interneurons

(A,B) In order to determine the percentage of cortical interneurons that express Sox6 at P21, telencephalic coronal sections from *Dlx5/6^{Cre};RCE^{EGFP/+}* mice were analyzed. (A) Within the somatosensory cortex 62±3% of the total number of interneurons (EGFP) express Sox6 (red). (B) A subset of hippocampal interneurons also express Sox6 (Box in panel B, shows a higher-power view of the region indicated). (C–F) To determine the percentage of each interneuron subtype that expresses Sox6, coronal sections of somatosensory cortex were analyzed at P21. (C–E) Representative examples of double immunostaining for Sox6 (red), and SST, PV or VIP (green). (C,D) The majority of PV and SST cells co-express Sox6. (E) We observed no colocalization between Sox6 (red) and VIP (green). (F) Shows the percentage of fate mapped *Dlx5/6, RCE* interneurons that express Sox6 (62±3%), and the percentages of specific cortical

interneuron subtypes that co-express Sox6 and the following markers: PV (93±4%); SST (94±6%); NPY (40±4%); and CR (19±2%). In contrast, VIP interneurons do not express Sox6 (2±1%). N=3 Scale bar in (A) corresponds to 40µm in A, 60µm in B, 50µm in C–E.

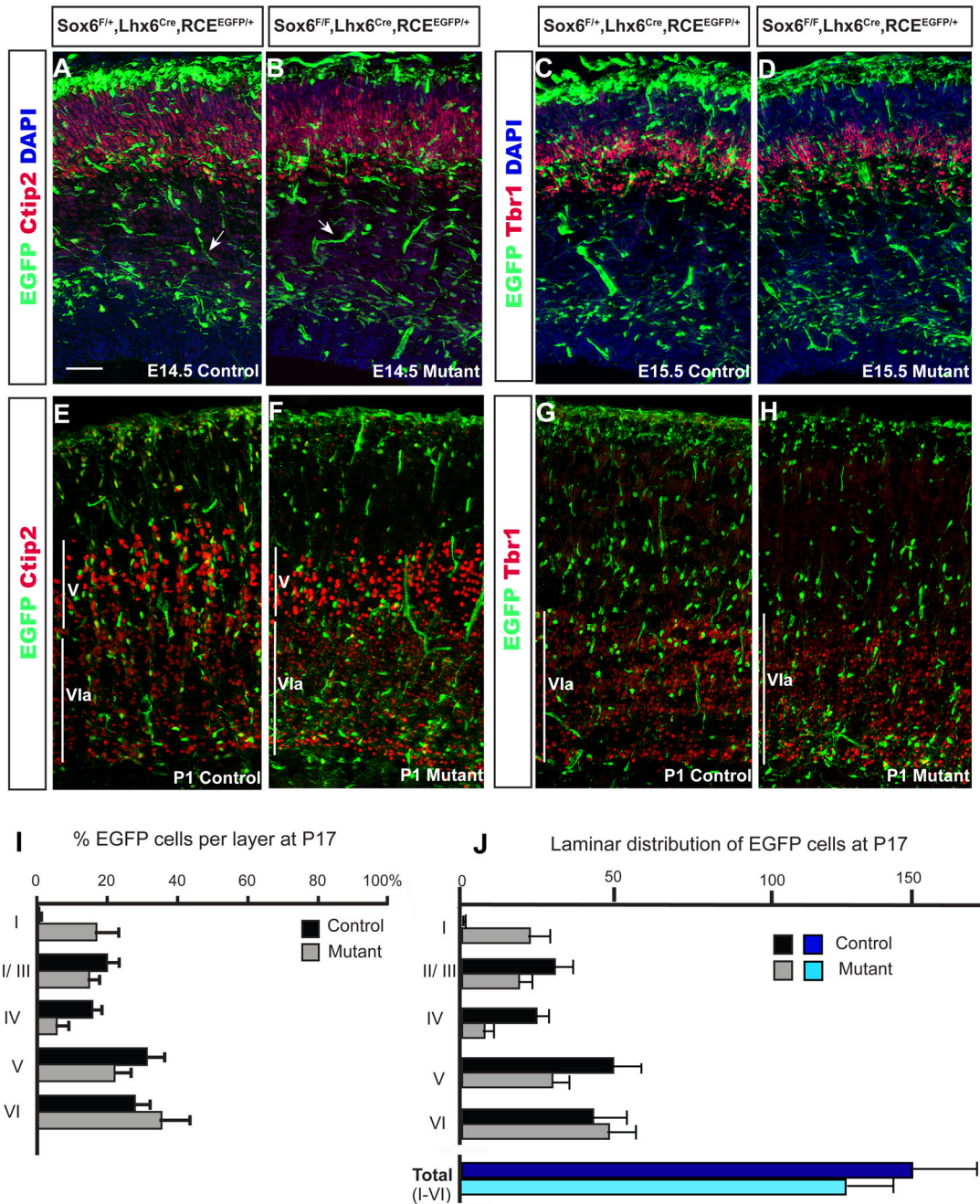


Figure 3. Sox 6 mutant MGE-derived interneurons have migratory defects resulting in them being largely restricted to the most superficial and deep cortical layers

(A,D) In order to determine if *Sox6* affects interneuron migration, we fate-mapped (A,C,E,G) *Sox6* control (*Sox6^{F/+};Lhx6^{Cre};RCE^{EGFP/+}*), and (B,D,F,H) mutant interneurons (*Sox6^{F/F};Lhx6^{Cre};RCE^{EGFP/+}*) during embryonic development (A–D) and at P1 (E–H). The specific cortical laminae were visualized using *Ctip2* (which is expressed in at high levels in layer V and weakly in layer VIa at perinatal ages; Arlotta et al., 2005; Chen et al., 2008) and *Tbr1* (which is expressed in layer VIa at perinatal ages; Hevner et al., 2001). While we did not detect a difference between control and mutant at E14.5 (A,B) or E15.5 (C,D); there was a noticeable difference in the distribution of *Sox6* mutant interneurons by P1 (E–H). *Sox6* mutant

interneurons accumulate in layer VI at the expense of the more superficial layers. This abnormal distribution persists at later times, with mutant *Sox6* interneurons preferentially occupying the superficial and deep cortical layers (layer I and VI, respectively), while being abnormally depleted in the intermediate cortical layers II–V (E–L). (E) The percentage of EGFP-expressing neurons in controls (black bars) and mutants (grey bars) in a given layer over the total number of EGFP in all layers at P17. Layer I: control ($0.5 \pm 0.3\%$) vs. mutant ($17 \pm 6\%$), Layer II/III: control ($20 \pm 3\%$) vs. mutant ($15 \pm 3\%$), Layer IV: control ($16 \pm 3\%$) vs. mutant ($5 \pm 3\%$), Layer V: control ($31 \pm 4\%$) vs. mutant ($22 \pm 5\%$), and Layer VI: control ($28 \pm 4\%$) vs. mutant ($36 \pm 8\%$). (F) Total number of EGFP cells per optical field. Layer I: control (0.7 ± 0.6) vs. mutant (22 ± 7), Layer II/III: control (30 ± 6) vs. mutant (18 ± 4), Layer IV: control (24 ± 4) vs. mutant (7 ± 3), Layer V: control (49 ± 9) vs. mutant (29 ± 5), and Layer VI: control (43 ± 11) vs. mutant (49 ± 9); and total (I–VI): control (158 ± 15) vs. mutant (130 ± 10). We analyzed three controls and three mutants at each of the timepoints examined: E14.5; E15.5 and P1. For the P17 analysis, we quantified the numbers of EGFP-expressing cells in the somatosensory cortices of four pairs of controls/ mutants. Arrow bars in (A–B) indicates blood vessels, which are labeled by the *Lhx6*^{Cre} driver (Fogarty et al., 2007). Scale bar in (A) corresponds to $200 \mu\text{m}$ in A–D and $150 \mu\text{m}$ in E–H.

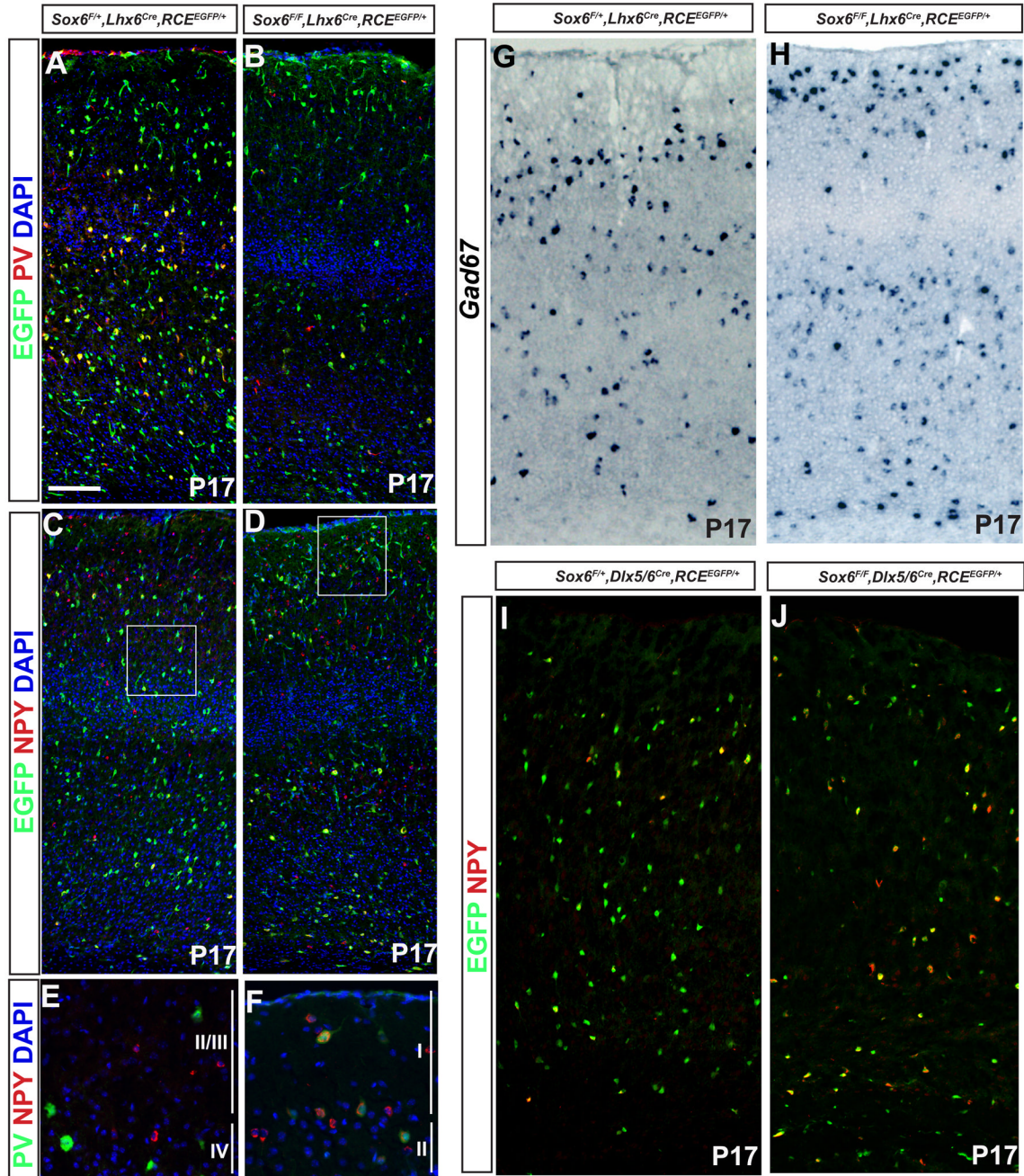


Figure 4. Effects of loss of *Sox6* gene function on cortical interneuron marker expression
 (A,B) Most of the *Sox6* mutant interneurons (*Sox6^{F/F};Lhx6^{Cre};RCE^{EGFP/+}*) lose PV expression, however a small percentage retain low levels of PV-expression, some of which become ectopically positioned in layer I. (C,D) By contrast, *Sox6* mutant interneurons upregulate NPY. (E) In the control brains (*Sox6^{F/+};Lhx6^{Cre};RCE^{EGFP/+}*) PV cells are distributed in layers II–VI (and absent in layer I), and a very low percentage of PV cells (green) co-express NPY (red) ($4\pm 2\%$). (F) In contrast, in mutant brains (*Sox6^{F/F};Lhx6^{Cre};RCE^{EGFP/+}*) some of the small amount of cells that keep low expression of PV are ectopically located in layer I. Virtually all the mutant PV expressing cells (green) also express NPY (red) ($93\pm 6\%$). E and F correspond to the squares in C and D, respectively. (G,H)

Gad67 expression was slightly decreased ($19\pm 11\%$). (I,J) To determine if the upregulation of NPY is confined to the interneuron population we performed NPY immunostaining (red) in *Dlx5/6* fate mapped interneurons (pan-cortical interneuron marker) in both (I) control (*Sox6^{F/+};Dlx5/6^{Cre};RCE^{EGFP/+}*), and (H) mutant (*Sox6^{F/F};Dlx5/6^{Cre};RCE^{EGFP/+}*) animals. We verified that the NPY upregulation in the mutant (J) is confined to the interneuron population (virtually all NPY expressing cells double label for EGFP). Quantification of the percentage of NPY expressing *Dlx5/6* fate mapped interneuron shows a vast increase of NPY expressing interneurons in the mutant ($72\pm 7\%$) (H); vs. in the control ($23\pm 5\%$). The percentage was calculated as a total number of NPY-EGFP expressing cells per total number of EGFP expressing cells. We used a total number of animals of five for (A–F), and three for (G–J). Countings were performed in the somatosensory cortex at P17–P19. Scale bar in (A) $70\mu\text{m}$ in (A–D), $8\mu\text{m}$ (E–F) and $50\mu\text{m}$ in (G–J).

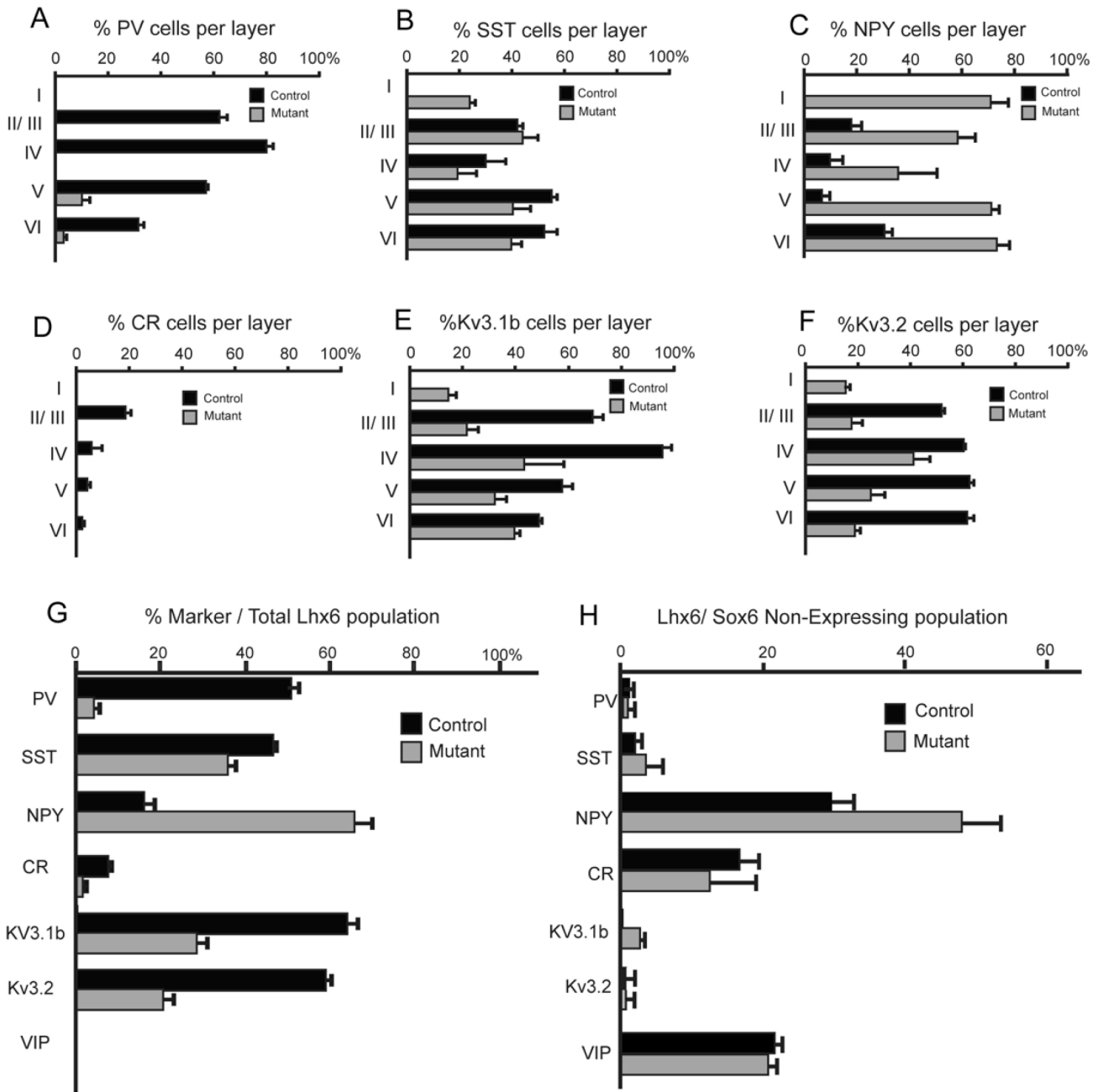


Figure 5. The cell autonomous and non-autonomous affects resulting from the loss of *Sox6* gene function on subtype-specific cortical interneuron marker expression

(A–H) To determine which markers are affected in *Sox6* mutant cells, we compared control (*Sox6*^{F/+};*Lhx6*^{Cre};*RCE*^{EGFP/+}) and mutant (*Sox6*^{F/F};*Lhx6*^{Cre};*RCE*^{EGFP/+}) animals at P17–P19. (A–F) Shows the percentage of fate mapped cells expressing a given marker relative to the total number of EGFP-positive neurons within that layer (marker-positive/EGFP-positive). The markers used were (A) parvalbumin (PV), (B) somatostatin (SST), (C) NPY, (D) calretinin (CR), (E) the voltage-sensitive potassium channel Kv3.1b, (F) the voltage-sensitive potassium channel Kv3.2. (G) Shows a summary of A–F showing the percentage of each marker examined, as a percentage of the total EGFP-positive cells within the somatosensory cortex

(layer I–VI). Note that while the markers PV, SST, CR, Kv3.1b and Kv3.2 are decreased, the marker NPY is increased. The extent to which individual markers are altered in the mutant differs in accordance with the layer examined (see A–F). (H) To determine the non-autonomous effects resulting from the loss of *Sox6* in non-MGE populations (i.e. those that are normally *Sox6*-negative) cortical interneurons, we compared control (*Sox6*^{F/+}; *Lhx6*^{Cre}; *RCE*^{EGFP/+}) and mutant (*Sox6*^{F/F}; *Lhx6*^{Cre}; *RCE*^{EGFP/+}) mice for the expression of the analyzed markers within the EGFP-negative population. Values were calculated by counting the total number of marker, EGFP-negative cells per optical section. Note that the only marker affected in this analysis was NPY, which was significantly increased.

All countings were performed at P17–P19 and bars correspond to stand error of the mean (N=5).

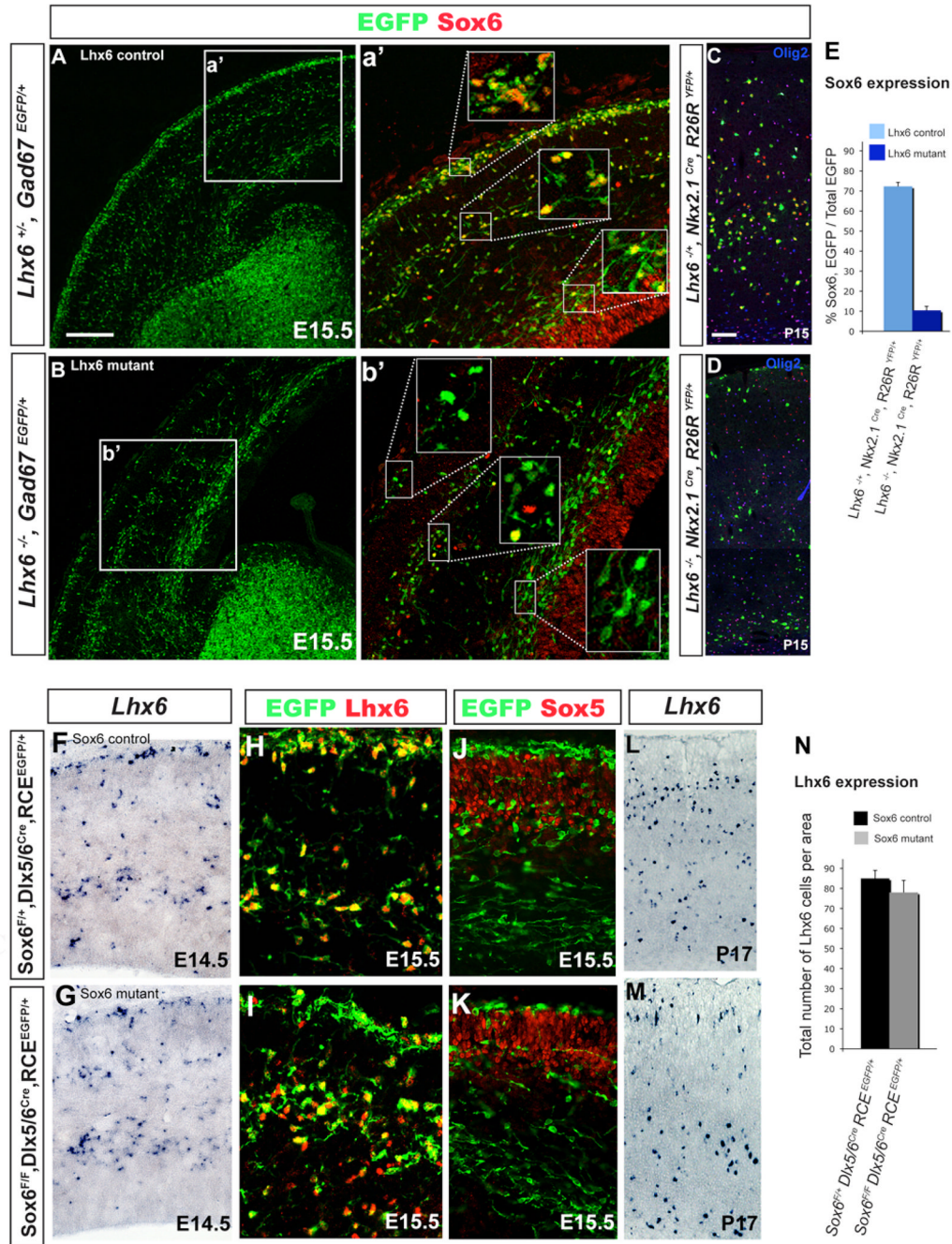
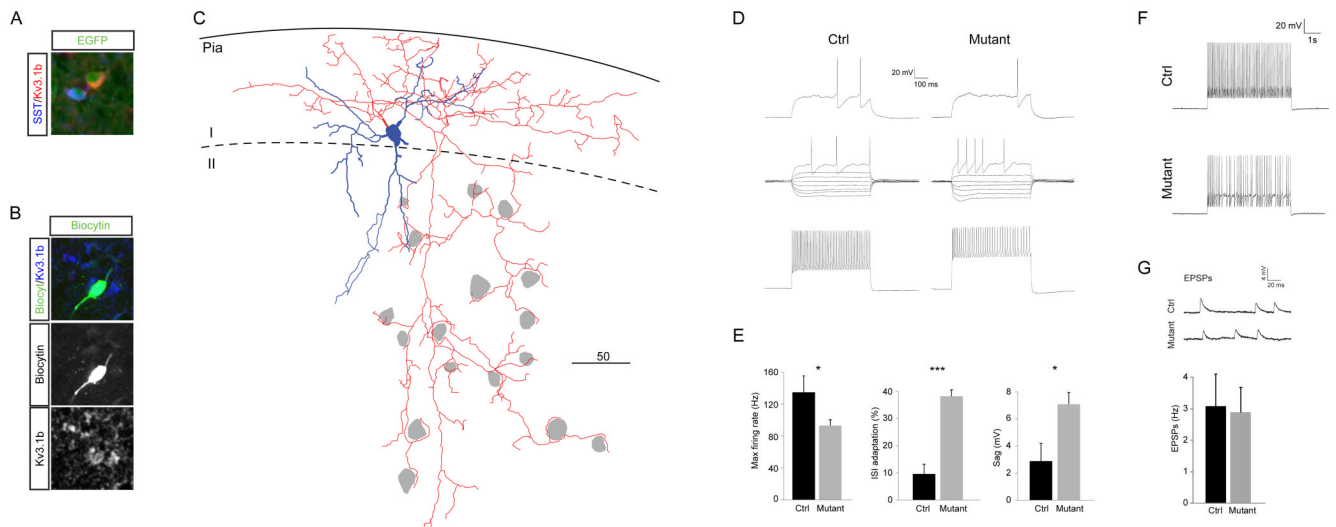


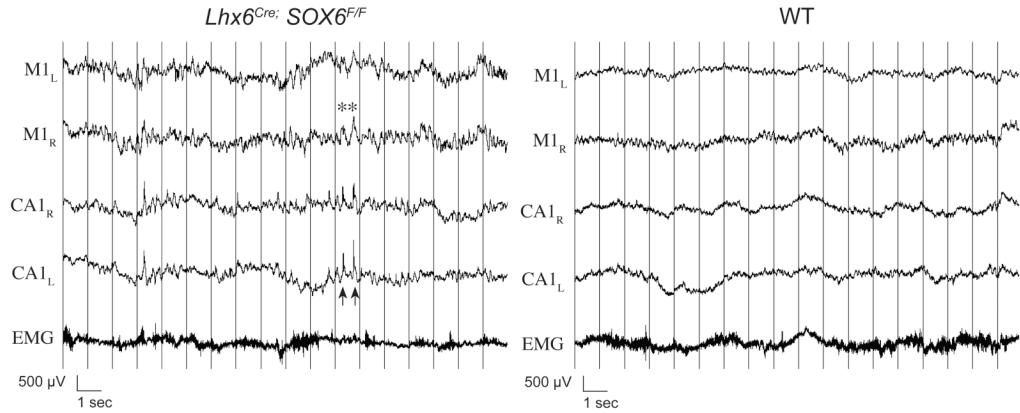
Figure 6. Sox6 is genetically downstream of Lhx6

To test the genetic relationship between *Sox6* and *Lhx6*, we both analyzed the expression of *Sox6* in *Lhx6* mutants (A–E), as well as the expression of *Lhx6* in *Sox6* mutants (F–N). *Sox6* expression is dramatically decreased in *Lhx6* mutant mice (*Lhx6*^{-/-}) at both E15.5 (A,B) and P15 (C,D). (A) In E15.5 control mice (*Lhx6*^{+/-}, *Gad6*^{EGFP}) migrating cortical interneurons (green) express *Sox6* (red), and this expression is dramatically decreased in mutant (*Lhx6*^{-/-}, *Gad6*^{EGFP}) mice (B). By contrast, *Sox6* cortical VZ expression is not affected in the *Lhx6* mutant. (C,D) A decrease of *Sox6* in *Lhx6* mutant interneurons is still observed at P15. In order to test the extent of the *Sox6* decrease in *Lhx6* mutant interneurons, we fate mapped MGE-derived interneurons by examining both (C) control (*Lhx6*^{+/-}; *Nkx2-1*^{Cre}; *R26R*^{YFP/+}),

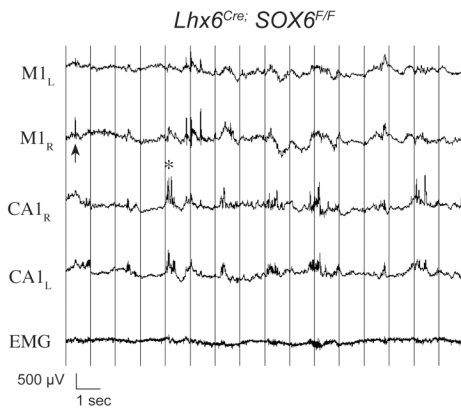
and (D) mutant ($Lhx6^{-/-};Nkx2-1^{Cre};R26R^{YFP/+}$) alleles with the $Nkx2-1^{Cre}$ driver. There was an obvious decrease in the expression of Sox6 in $Nkx2-1$ fate mapped $Lhx6$ mutant cells, while there was no change in Sox6 expression in Olig2-expressing non-neural cells. (E) Shows the percentage of Sox6-expressing interneurons in fate mapped $Nkx2-1$ -lineage interneurons, as calculated as the ratio between the number of cells that are Sox6 positive/YFP double-positive as a percentage of the total number of YFP fate mapped cells, in either $Lhx6$ control ($72\pm 2\%$) in $Lhx6^{+/-};Nkx2-1^{Cre};R26R^{YFP/+}$ or mutant ($10\pm 2\%$) in $Lhx6^{-/-};Nkx2-1^{Cre};R26R^{YFP/+}$ mice. (F–N) $Lhx6$ expression is not affected in Sox6 mutant cells. (F–I) We saw no difference between E14.5 controls ($Sox6^{F/+};Dlx5/6^{Cre};RCE^{EGFP/+}$) and mutants ($Sox6^{F/F};Dlx5/6^{Cre};RCE^{EGFP/+}$) in $Lhx6/Lhx6$ expression as assessed by *in situ* (F–G) and antibody staining (H,I). Similarly, we saw no difference in the expression of Sox5 in control versus mutant mice (J,K). (L,N) $Lhx6$ expression was still largely unaltered at P17. (N) $Lhx6$ expression was calculated as the total number of $Lhx6$ -expressing cells at P17 in both the control ($85\pm 4\%$) in $Sox6^{F/+};Dlx5/6^{Cre};RCE^{EGFP/+}$ and mutant ($78\pm 6\%$) in $Sox6^{F/F};Dlx5/6^{Cre};RCE^{EGFP/+}$ mice. Scale bar in (A) corresponds to $300\mu\text{m}$ in A and B. Scale bar in (C) corresponds to $50\mu\text{m}$ in C and D, $25\mu\text{m}$ in F–J and $40\mu\text{m}$ in L and M.



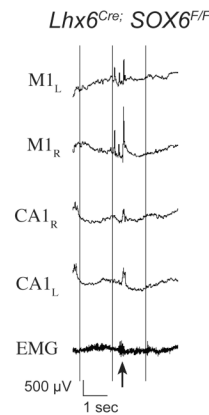
A) Wake exploration



B) Sleep: interictal epileptic activity



C) Myoclonus



D) Seizure

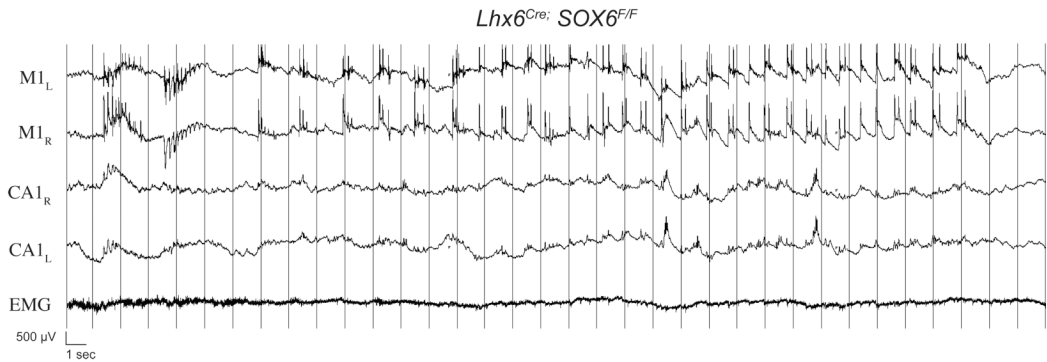


Figure 8. EEG characterization

A) Mutant P16 EEG recordings in cortical fields (M1) reveal dysrhythmic theta oscillations interrupted by high amplitude delta waves (asterisk) often associated with hippocampal epileptic discharges in CA1 (arrows).

B) Interictal epileptic activity becomes more prominent during slow wave sleep with independent discharges in the cortex (arrow) and hippocampi (asterisk).

C) Although usually asymptomatic and considered interictal, simultaneous epileptic discharges in the hippocampi and polyspike complexes in the cortex occasionally manifest as generalized myoclonus.

D) Generalized seizures with synchronous bi-frontal onset often remain confined to cortical fields, with variable hippocampal involvement.
(Acquisition: 2000Hz, HP 0.1 Hz, LP 300 Hz, filtered at LP 70Hz for display)

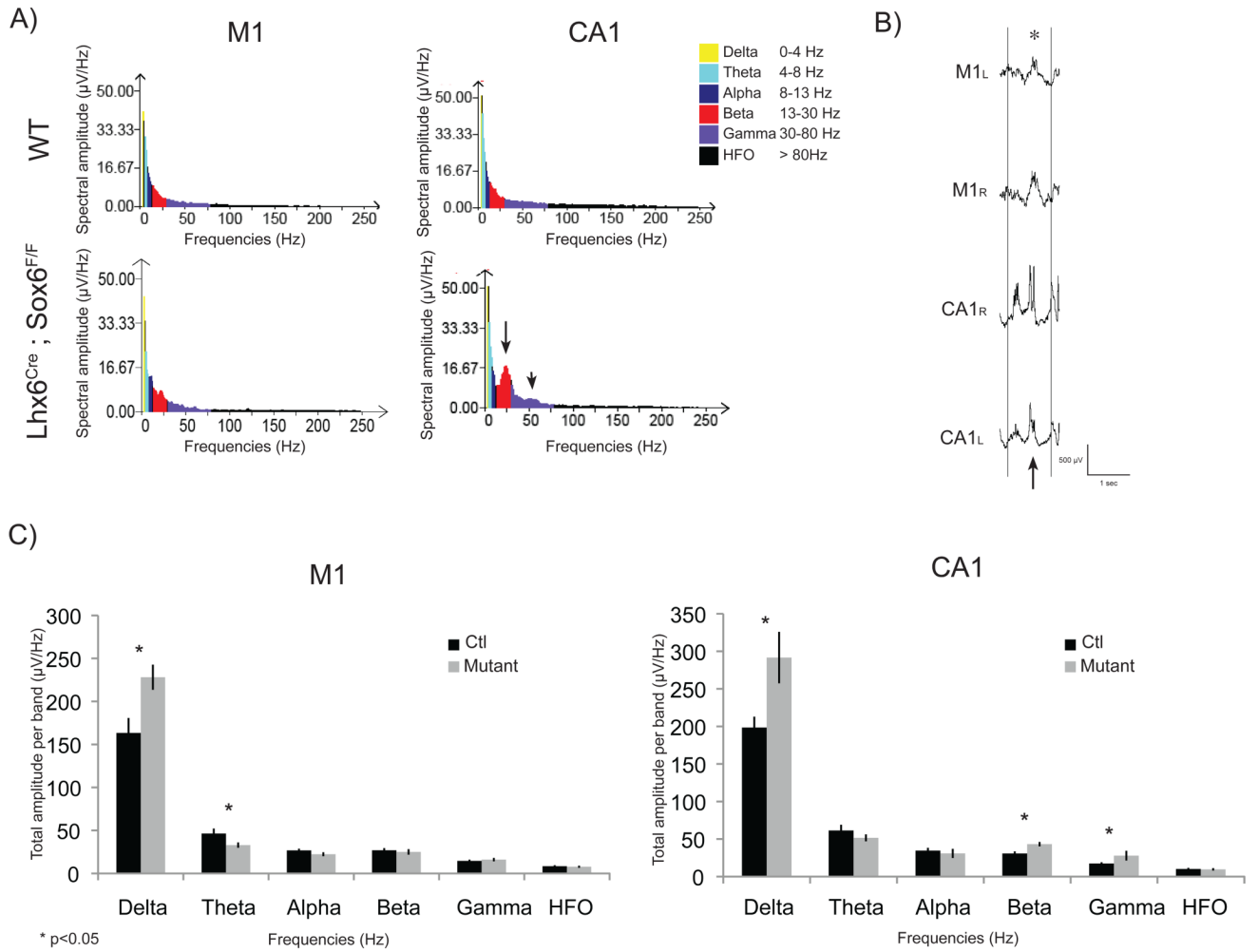


Figure 9. Spectral Analysis

Spectral analysis (FFT: consecutive 1 sec segments, averaged over six 10 sec epochs) during slow wave sleep at P17 ($\pm 0.5D$) reveal spectral band amplitude (sq root power) modifications with increased delta power band and decreased theta power band in cortical EEG (A+C) reflecting frequent high amplitude delta waves (B, asterisk). In addition, delta, beta and gamma powers were increased in hippocampal recordings (A arrows: additional peaks at $25.5 \pm 5Hz$ and minor peak at $53 \pm 3Hz$, Averaged power increase: C) reflecting frequent epileptic bursts composed of high amplitude delta waves with superimposed polyspikes (B, arrow).